CONSTANŢA „OVIDIUS'' UNIVERSITY
DOCTORAL SCHOOL
FACULTY OF MEDICINE
DISCIPLINE: PATHOLOGY

MORPHOLOGICAL COMPARATIVE STUDY OF PROSTATE ADENOCARCINOMA WITH LESIONS THAT MIMIC MALIGNANCY

ABSTRACT

SCIENTIFICAL COORDINATOR
PROF.UNIV.DR. MARIANA AŞCHIE

PH.D. CANDIDATE
MANUELA IFTIME (ENCIU)

CONSTANŢA
2012

CONTENTS

Abrevieri

A – atrophy

ADK – adenocarcinoma

AN – nuclear area

AS – sclerosing adenosis

CEA – carcinoembryonic antigen

CKHMW – high molecular weight cytokeratin

CT –transitional carcinoma

Deq – mean diameter

Dmax – maximum diameter

Dmin - minimum diameter

LG-PIN – low grade prostate intraepithelial neoplasia

HAA – atypical adenomatous hyperplasia

H&E – Hematoxilin – Eosin

CNE –neuro-endocrine carcinoma

E - elongation

HG-PIN - high grade prostate intraepithelial neoplasia

ICN – nonspecific chronic inflammation

IGN – nonspecific granulomatous inflammation

ISUP – International Society of Urological Pathology

IX – xantogranulomatous inflammation

LMADK – mimic adenocarcinoma lesions

OMS – World Health Organization

SMA – smooth muscle actin

CB – basaloid carcinoma

CK7 – cytokeratin 7

CK20 – cytokeratin 20

HCCC – clear cell cribriform hyperplasia

HCB – basal cell hyperplasia

HBP – benign prostatic hyperplasia

HPF – high power field

P –nuclear perimeter

PSA –prostatic specific antigen

PSMA - prostate specific membranous antigen

PAP – prostate acide phosphatase

PTI – inflammatory pseudotumour

r - Pearson correlation coefficient

std – standard deviation

TURP – Transurethral resection of prostate

PIN – prostate intraepithelial neoplasia

Key words: adenocarcinoma, lesions that mimic malignancy, architecture, immunohistochemistry, morphometry

Introduction

Adenocarcinoma of the prostate is the most common malignancy of the prostate. Malignant prostate neoplasia is ranked first of the prevalence of cancers and represents the second cause of cancer mortality in the males after lung cancer. It is also characterized by several features: develop on a hormone-dependent organ, which is the intersection of urogenital system, and is characterized by lymphatic and bone spread. Risk of disease vary by age. About 75% of men diagnosed with prostate cancer were older than 65 years although the disease has been diagnosed in young adults and even children.

The aim of this study is attributed to the fact that in the Service of Pathology where I work every year more than 400 lesions of the prostate are diagnosed (1823 cases in four years). In the period 2008-2011, 365 cases were diagnosed adenocarcinoma and noticed a gradual increase in the number of cases, their number doubling in 2011 compared to 2008.

Also in current medical practice, I noticed that most problems of differential diagnosis are lesions that mimic adenocarcinoma, which were represented by 283 cases. This group brings together a number of benign lesions presenting structural similarities with adenocarcinoma and whose differentiation is usually extremely difficult on their staining routine. Between 2008-2011 the two lesions undergo a progressive increase in the number of cases until 2011, when the number of mimickers is higher. Diagnosis is more difficult, as these diseases are accompanied by elevated prostate specific antigen levels.

Most benign lesions were represented by small glandular proliferation consisting of atypical adenomatous hyperplasia, atrophy, basal cell hyperplasia, sclerosing adenosis, but also histoanatomial structures such as Cowper glands. Of these lesions, the most common was atypical adenomatous hyperplasia potentially a precursor to adenocarcinoma transitional zone which in 2011 presented a number of cases by 2.5 times compared to previous years. From this emerges the importance of finding statistical comparative study of these pathologies.

In addition, inflammatory processes such as granulomatous prostatitis and xantogranulomatoasă can simulate a high-grade adenocarcinoma. Clear cell cribriform hyperplasia may be confused with a large gland adenocarcinoma.

Often are necessary special techniques of immunohistochemistry to highlight the benign nature of these entities and to avoid a false positive diagnosis of cancer, with important consequences for both the patient's mental state, but also on the costs and adverse effects of treatment. Thus, if cancer receive surgical treatment, radiotherapy, hormone therapy, the patient followed is recommended in mimic lesions. Knowing the different histological features and changes in the prostate that causes disease process may have an important role in understanding the spectrum of lesions, the choice of the most appropriate and early therapies that are available.

The goal of the study is to provide a thorough research in comparing the histopathological parameters, morphometric and mean PSA values of the two entities and to define clear criteria morphology, in order to achieve the differential diagnosis between prostate adenocarcinomas and

lesions that mimic adenocarcinoma. Also, another aim was represented by the frequency of these entities for a period of 4 years from all spectrum of prostate lesions.

The paper is structured in two parts, divided into 11 chapters. The first part contains data from the literature on embryology, anatomy, histophysiology and epidemiology, histopathology findings of prostate cancer and lesions that mimic adenocarcinoma. The second part refers to my own contributions to the study of morphological study of adenocarcinomas and lesions that mimic adenocarcinoma summarized in five chapters. This study has resulted in a diagnostic protocol of the two groups of lesions. For this study and to have a reference point to compare the results obtained have been consulted a number of 378 titles. This paper has a rich iconography, represented by 299 figures, of which 30 are graphs, 219 original macroscopic and microscopic images, 50 by general part and 106 tables.

Material and methods

This study was conducted over a period of four years, between 2008-2011, in the Department of Clinical Pathology Constanta County Emergency Hospital. In order to realize this work were analyzed patients admitted with presumptive diagnosis of prostate tumors in Urology department in Constanta County Emergency Hospital from the 1 January 2008-31 December 2011. Patients group hospitalized with the presumptive diagnosis of prostate tumors treated surgically and receiving histopathological diagnosis was represented by 1823 cases.
Distribution of cases according to histological diagnosis is systematized in the following table:

Table nr. XVIII Distribution of cases by histological type between 2008-2011

Cases assessed	Histopathologycal type	Number of cases according to histological type	Percent
1823 patients surgically treated with histopathological exam	ADK	**365**	20,02 %
	transitional cell carcinoma	13	0,71 %
	Lesions that mimic adenocarcinoma	**283**	15,52 %
	PIN	148	8,12 %
	Benign hyperplasia	1014	55,62 %

Selection of studied cases

To achieve the differential diagnosis of adenocarcinomas with lesions that mimic prostate adenocarcinoma, I used several criteria for inclusion and exclusion of cases.

Criteria for inclusion of studied cases:

- We selected 69 cases of acinar adenocarcinoma Gleason grade 1 and 2 to study morphometric and structural parameters for small gland adenocarcinomas; we did not realize

morphological study of malignant neoplastic glandular structures corresponding to the prostate tissue with largest contingent. In this group we included two cases of atrophic adenocarcinoma.

- To study morphometric and structural parameters of adenocarcinomelor with large gland architecture we selected only cases with large glands, cribriforme, papillary and comedonecrosis. This is represented by 39 cases consisting of: 19 adenocarcinoma Gleason grade 3 cribriform-papillary type (Gleason score 3+3), 10 cases of Gleason grade 4 cribriform adenocarcinoma and 10 cases of Gleason grade 5, comedonecrosis type. We did not realize morphological study of malignant neoplastic glandular structures corresponding to the prostate tissue with largest or smaller contingent.
- For architectural type fused glands we have selected 33 cases of acinar adenocarcinoma Gleason grade 4, fused glands guy and clear cell (Gleason score 4 +4) ; we did not realize morphological study of malignant neoplastic glandular structures corresponding to the prostate tissue with largest or smaller contingent.
- cases of acinar adenocarcinoma with solid architecture consisting of adenocarcinomas composed of Gleason grade 5 (Gleason score 5 +5), (30 cases). We did not realize morphological study of malignant neoplastic glandular structures corresponding to the prostate tissue with largest or smaller contingent.
- Case of bazaloid prostate carcinoma, for comparison with basal cell hyperplasia.
- a control group, represented by cases diagnosed with benign prostatic hyperplasia, adenomatous component, we evaluated the nuclei of epithelial component for morphometric study (30 cases)
- cases diagnosed with simple atypical adenomatous hyperplasia (60 Cases); we did not realize morphological study on prostate tissue fragments diagnosed with HAA who had associated injuries
- Cases diagnosed with prostate atrophy (19)
- Cases diagnosed with basal cell hyperplasia (21)
- cases diagnosed with sclerosing adenosis (33)
- ses diagnosed with clear cell cribriform hyperplasia (4)
- Cases of xantogranulomatous inflammation (7)
- Cases of nonspecific granulomatous inflammation (7)
- Cases diagnosed with nonspecific chronic inflammation (42)
- the case diagnosed with inflammatory pseudotumour, for comparison with solid adenocarcinomas

Exclusion criteria:

- Patients with carcinoma of the prostate transitional
- Squamous carcinoma of the prostate
- Ductal, mucinous and neuro-endocrine adenocarcinomas
- Forms associated adenocarcinoma
- Cases diagnosed with intraepithelial neoplasia

Thus, morphological study was conducted on a group of cases, consisting of 373 cases.

Study groups represented by adenocarcinomas and corresponding pseudoneoplazic lesions were summarized in the following table:

Table no. VII The control group

Control Group	No. cases
benign prostatic hyperplasia, adenomatous component	30

Table no. VIII Group represented by small glands architecture

small glands architecture	No. cases
Adenocarcinomas	69
Atypical adenomatous hyperplasia	60
Sclerosing adenosis	33
Atrophy	19
Basal cell hyperplasia	21
Cowper glands	10
Basaloid carcinoma	1

Table no. IX Group represented by large glands architecture

large glands architecture	No. cases
Adenocarcinomas	39
Clear cell cribriform hyperplasia	4

Table no. X Group represented by fused glands architecture

fused glands architecture	No. cases
Adenocarcinomas	33
xantogranulomatous inflammation	7

Table no. XI group represented by solid architecture

Solid architecture	No. cases
Adenocarcinomas	30
nonspecific granulomatous inflammation	7
nonspecific chronic inflammation	42
inflammatory pseudotumour	1

Comparative evaluation of adenocarcinomas and lesions that mimic malignancy based on a working scheme

To achieve differential diagnosis with pseudoneoplastic lesions we used as reference architecture glands. Depending on this, we grouped adenocarcinomas into four architectural types based on the size and shape of glands:

- Small glands arhitecture
- Large glands arhitecture
- fused glands architecture
- Solid architecture

This classification was based on the original diagram Gleason [1,2]. The prototype of differential diagnosis based on glandular architecture and Gleason score was published by Srigley in 2004 and

its work plan formed the basis in order to achieve differential diagnosis in this study [3]. Because division by architectural type of Srigley study was conducted in 2004, we adjusted the work diagram a ccording to 2005 ISUP modified Gleason score [4].

Table no. XIII prostate adenocarcinoma classification architecture based on 2005 ISUP modified Gleason score

Adenocarcinoma arhitecture	Gleason Grade
Small glands	1 2
Large glands	cribriform or papillary 3 cribriform 4 comedonecrosis 5
Fused glands	Fused type 4 Clear cell (hipernefromatoid) 4
Solid arhitecture	5 absence of glandular differentiation

On the basis of lesions diagnosed in Constanta Clinical Pathology Service, we have developed the following scheme for the differential diagnosis of adenocarcinoma with mimic lesions architecture based on arhitectural type:

Table no. XIV Benign lesions that mimic adenocarcinoma

Arhitectural type of glands in adenocarcinoma	Pseudoneoplastic lesions
Architecture represented by small glands	Cowper Glands
	Atrophy
	Basal cell hyperplasia
	Sclerosing adenosis
	Atypical adenomatous hyperplasia
Architecture represented by large glands	Clear cell cribriform hyperplasia
Architecture represented by fused glands	xantogranulomatous inflammation
Solid architecture	nonspecific chronic inflammation with artifacts
	nonspecific granulomatous inflammation
	inflammatory pseudotumour

Morphological and immunohistochemical methods for the examination of preparations

Studied cases were assesed by macroscopic, microscopic, immunohistochemical and morphometric point of view. Have been analyzed surgical specimens obtained by transurethral resection of the prostate and prostatectomy. Surgical pieces were subjected to macroscopic examination first.

Subsequently, the pieces were processed through successive stages until histological slide stage. The specimen was fixed in 10% formalin for 24 hours and were included in blocks and dehydrated in acetone solution for 24 hours. Sections with a thickness between 4 and 6 microns were stretched on slides and for deparaffination were placed in methanol. The sections thus obtained were stained

with Hematoxylin-Eosin and van Gieson. The process has been completed with preparation clarifying and mounting slide.
The microscopic preparations thus obtained were examined to a Nikon E600 microscope.

Immunohistochemistry techniques

In order to establish the diagnosis has been used immunohistochemistry techniques - En Vision procedure (Dako) [5]. Following antibodies were applied :

- monoclonal Mouse Anti-Human Prostate Specific Antigen, clone ER-PR 8, isotype IgG1, Kappa (DAKO)
- monoclonal Mouse anti-Human High Molecular Weight Cytokeratin, Clone 34βE12, Isotype IgG1, Kappa (DAKO)
- monoclonal Mouse Anti-Human – CD68, clone EBM11, Isotype IgG1, Kappa; (DAKO);
- monoclonal Mouse Anti-Human – CD45 (Leukocyte common antigen), clone 2B11+PD7/26, Isotype IgG1, Kappa+IgG1, Kappa; (DAKO);
- monoclonal Mouse Anti-Human – Ki-67, clone MIB-1, Isotype IgG1, Kappa; (DAKO);
- monoclonal Mouse Anti-Human – SMA (smooth muscle actin), clone 1A4, Isotype IgG2a, Kappa [5,6], (DAKO);

Qualitative assessment of architectural parameters

To achieve the differential diagnosis of small glands architecture we evaluated t several parameters, which are presented in the following table:
Structural parameters evaluated are presented in the following table:

Table no. XVI Parameters assessed to the group with small glands architecture

parameters that assess architecture of the lesion	Lesion diameter
	Number of glands
	Lobular pattern
	Pleomorphism of the glands
	Distance between glands
	presence of a central duct
	Periglandular halo
glandular parameters	Luminal side shape
	intraluminal content
immunohistochemical aspects	presence of basal cells (34βE12)

To differentiate prostate adenocarcinomas by solid architecture with large glands fused glands, architectural parameters were not found to be important, which is why they have not been applied and determined.

Morphometric study

For a more detailed assessment of epithelial component, we used morphometric semiautomatic method**.** Measurements was performed using Lucia Net software computer-assisted imaging system consisting of a Nikon light microscope, a digital camera and image acquisition digital camera Nikon DN 100, with a resolution of 1280-1024 pixels. For each case, 100 nuclei were outlined, every 10 nuclei in 10 fields. Nuclear outline was traced to a magnification of 400.
Previously, the software was calibrated for the objective used. Measurement unit was μm. The following parameters were assessed:

- AN nuclear area (μm²) and standard deviation dst NA;
- nuclear perimeter (μm) and standard deviation dst P;
- Elongation factor E and standard deviation dst E (this is a factor which reflects the shape of nuclei ; for spherical nuclei has the value 1, and for ellipsoidal shape of nuclei, its value increases).
- Deq – mean diameter
- Maximum diameter Dmax and Dmax dst standard deviation;
- Mininum diameter Dmin and standard deviation of minimum diameter Dmin dst.

Statistical study

Statistical analysis of data was performed using Microsoft Excel 2007 and medical statistics software MedCalc for Windows, version 12.2.1.0, trial. For each quantitative value was determined mean value and standard deviation. For data processing we used student test (t-test) and $\chi 2$ test for the dichotomous variables. Results were considered statistically significant at a p-value <0.05.
In order to establish correlations between morphometric parameters, we determined the Pearson correlation coefficient (r).

Histopathological and immunohistochemical comparative evaluation of adenocarcinomas with lesions that mimic malignancy

Comparative evaluation of lesions including small glands

Results and discussion of parameters evaluated between adenocarcinomas and atypical adenomatous hyperplasia small glands

Atypical adenomatous hyperplasia is a proliferative lesion composed of circumscribed nodules composed of small glands, crowded and often simulating small gland adenocarcinoma (Gleason grade 1 or 2). Prostate adenocarcinoma Gleason grade 1 is composed of small glands looking uniform and showing minimal stromal invasion. Adenocarcinoma Gleason grade 2 is characterized by infiltrative margins and a slight variation in the size of glands compared with Gleason grade 1 according to Gleason grading [7,8]. A reference study of this work was made by Ahmed Midi in 2008 [9], which conducted a comparative study of the structural characteristics developed in both entities. My goal is to compare some of the parameters used to it, in conjunction with morphometric study in order to determine the parameters of differentiation. By studying prostate pathology casework between 2008-2011, HAA had a frequency of 11.24%.
Values obtained by evaluation of architectural parameters, are presented in the following table:

Table no. XXXIX Comparison between HAA and small glands adenocarcinoma architectural parameters

Parameter	Evaluation criteria	Number of HAA cases	Number of ADK cases	Test	p
Focus diameter	-	2,14±0,52	3,34±2,34	t-	p<0,05

				test	
Number of glands	10-30	34	0	t-test	p<0,05
	30-50	24	56		
	>50	2	13		
Central duct	Present	45	0	χ^2	p<0,05
	Absent	15	69		
Lobular pattern	Absent	10	60	χ^2	p<0,05
	Present	50	9		
Pleomorphism of the glands	Absent	1	19	χ^2	p>0,05
	Slightly	20	23		
	Marked	25	27		
Distance between glands	Absent	37	40	χ^2	p>0,05
	Minimum (1-3 cells)	23	29		
	Marked (peste 3 cells)	0	0		
Periglandular halo	Present	0	0	χ^2	p>0,05
	Absent	60	69		

The results were statistically significant in the average size of foci studied ($p < 0.05$). We found that foci diameter of AAH are smaller than those of ADK, as in the study by Ahmed Midi in 2008, but his study results were not statistically significant. This may explain the study material obtained by transurethral resection for me. Lobulated appearance was seen at a rate of 83.33% for HAA to 13.04% for adenocarcinomas. However, lobulated appearance was seen in 9 cases of adenocarcinoma. The results were statistically significant.

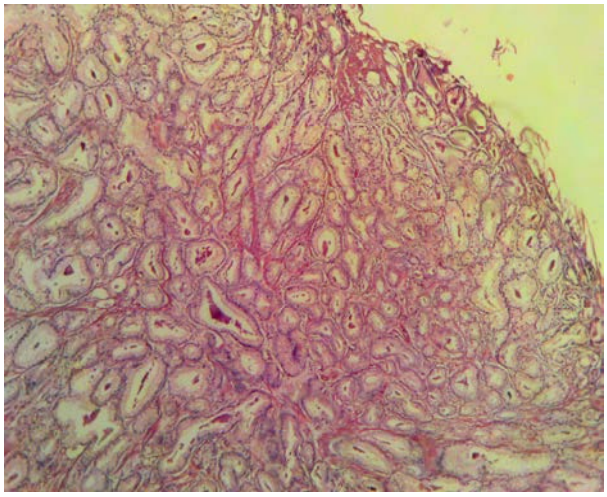

Fig. 144 Adenocarcinoma - slightly glandular pleomorphism, H&EX100 (original)

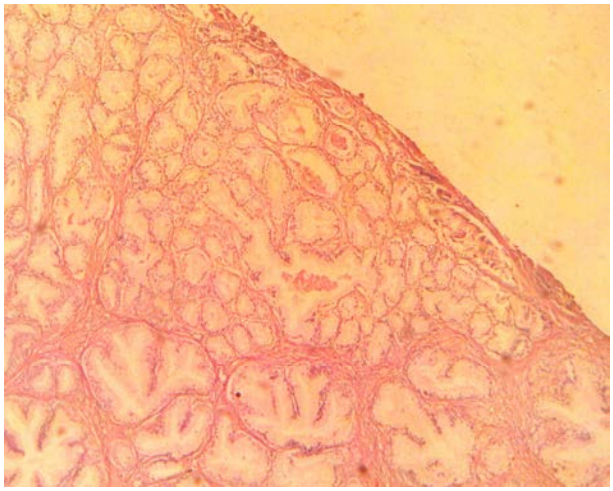

Fig. 133 Circumscribed nodule (lobulated appearance) atypical adenomatous hyperplasia, H&Ex40, (original)

The central duct was identified in 75% of cases of HAA and was a feature absent in adenocarcinomas. The results were statistically significant. The results are similar to other studies [10.11].

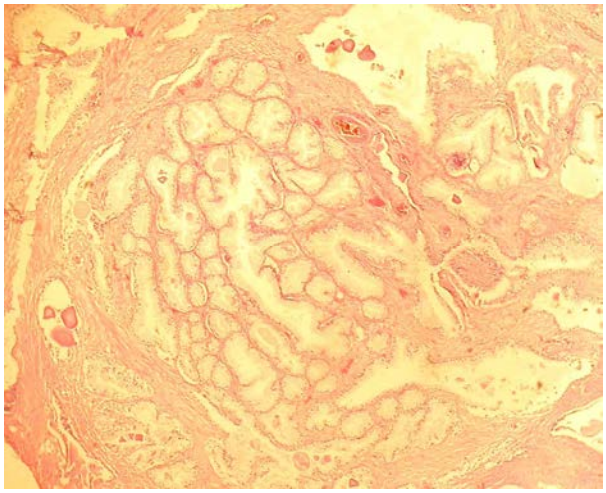

Fig. 138 Atypical adenomatous hyperplasia - the presence of a central duct and absence of intraglandular content H & EX100 (original)

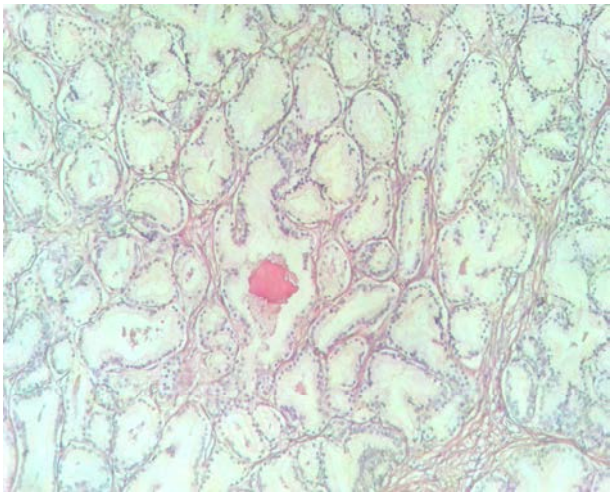

Fig. 136 Atypical adenomatous hyperplasia - the presence of a central duct and intraluminal crystalloids; H&EX100 (original)

We found that most cases of HAA containing corpora amilacei (75%), while cristaloids prevailing in the lumen of adenocarcinomas (75.36%). Amilacei corpora presence in benign lesions is probably a consequence of congestion and stasis secretion [12]. They correlate with symptoms of urinary obstruction and patient age.

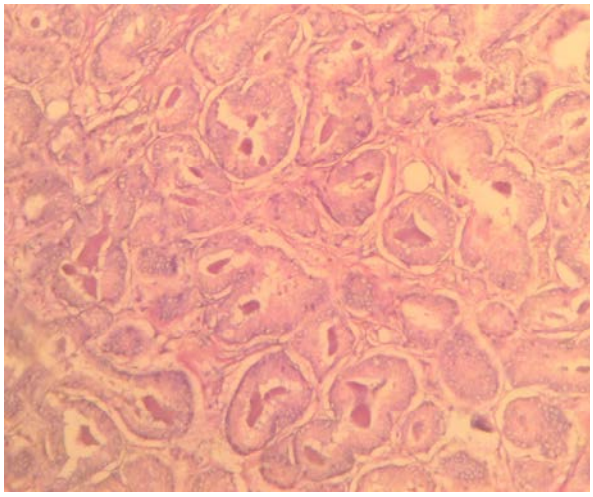

Fig. 143 Gleason grade adenocarcinoma 2 - presence of crystalloids and minimum distance between glands, H&EX100 (original)

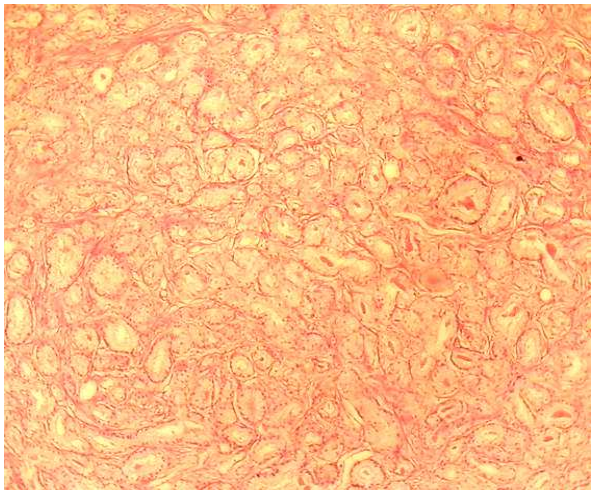

Fig. 148 Atypical adenomatous hyperplasia - nodules well defined, slightly pleomorphism, H & Ex40, (original)

Discontinuous basal cells were present in the entire group of HAA, while adenocarcinomas showed a 100% negative reaction 34βE12, at the level basal cells were absent. The results were statistically significant ($p < 0.05$).

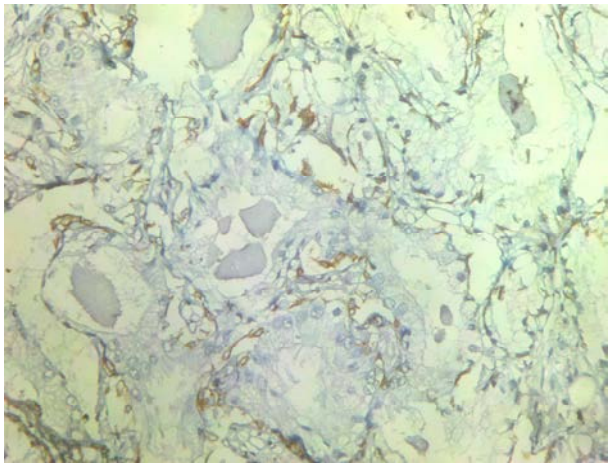

Fig. 149 Atypical adenomatous hyperplasia - discontinuous immunostaining to 34βE12x200 (original)

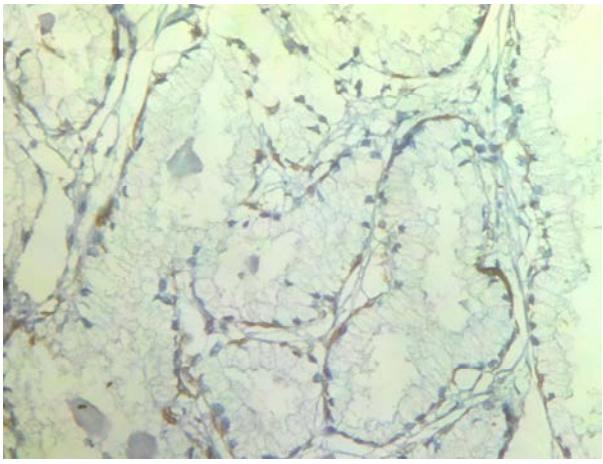

Fig. 150 Atypical adenomatous hyperplasia - discontinuous positive immunoreaction to 34βE12x200, (original)

Results and discussion of parameters evaluated between adenocarcinomas with small glands and sclerosing adenosis

Of the 1823 transurethral prostate resections made between 2008-2011, sclerosing adenosis had a frequency of 1.81%.

Table XLII Frequency of sclerosing adenosis at international level

Referenced studies	Year	Incidence
Bostwick DG, Cheng L	2008	2%
Grignon DJ et al	1992	2%
Sakamoto N	1991	1,9%

Diameter foci in sclerosing adenosis had an average of 2.27 mm, ranging from a minimum of 1 mm to 2.5 mm maximum. The results were statistically significant. The data obtained are slightly lower than those of Cheng Liang's study in 2010, where mean value was 5 mm, and ranged between 1.5 and 18 mm [13].

Table no. XLIV Comparison between architectural parameters of AS and ADK with small glands

Parameter	Evaluation criteria	Number of ADK cases	Number of AS cases	Test	p
Focus diameter	-	3,34±2,34	2,27±0,45	t-test	p<0,05
Number of glands	10-30	0	18	t-test	p<0,05
	30-50	56	15		
	>50	13	0		
Lobular pattern	Absent	60	13	$\chi 2$	p<0,05
	Present	9	20		
Central duct	Absent	69	33	$\chi 2$	p>0,05
	Present	0	1		
Pleomorphism of the glands	Absent	19	3	$\chi 2$	p>0,05
	Slightly	23	25		
	Marked	27	5		
Distance between glands	Absent	40	18	$\chi 2$	p>0,05
	Minimum (1-3 cells)	29	13		
	Marked (more than 3 cells)	0	2		
Periglandular halo	Present	0	25	$\chi 2$	p<0,05
	Absent	69	8		

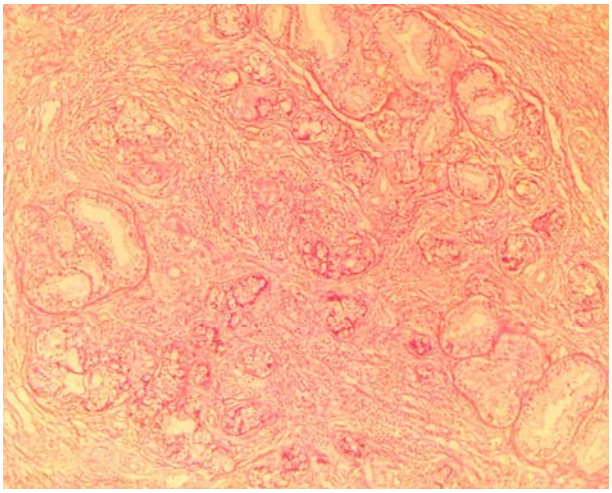

Fig. 153 Sclerosing adenosis - lobulated appearance, H&EX100 (original)

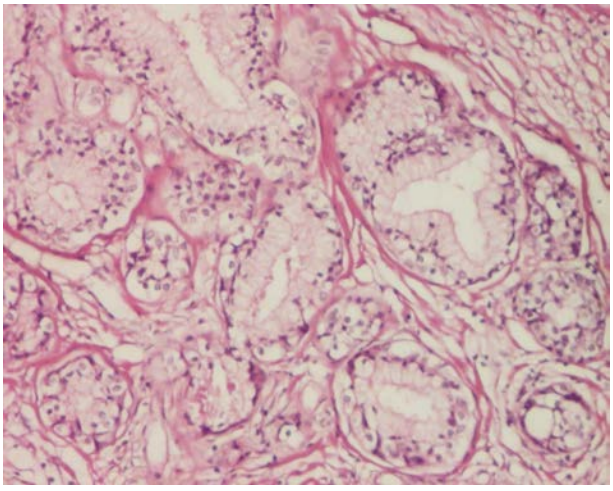

Fig. 160 Sclerosing adenosis– marked glandular pleomorphism and periglandular eosinophilic halo, H&EX100 (original)

Lobulated pattern was identified in 60.6% of the AS group compared with 13.94% of adenocarcinomas. The results were statistically significant. Regarding the glandular pleomorphism, the results were not statistically significant. An explanation of this result is because the group of adenocarcinomas with small glands included Gleason grade 2 adenocarcinomas, which are more lax and less uniform glands, so that the shape is not specific.

Eosinophilic periglandular halo was found in 75.75% of sclerosing adenosis studied and was absent in adenocarcinomas. The results were statistically significant. In this study, three cases of AS showed a positive reaction to 34βE12 discontinuous basal cells, the majority (30 cases) showing a continuous imunostaining. A total of 30 cases was positive for SMA. Suzuki Y et al also found myoepithelial differentiation of the three cases studied, basal cells were characterized by positivity for SMA, S100 and negative PSA at this level [14].

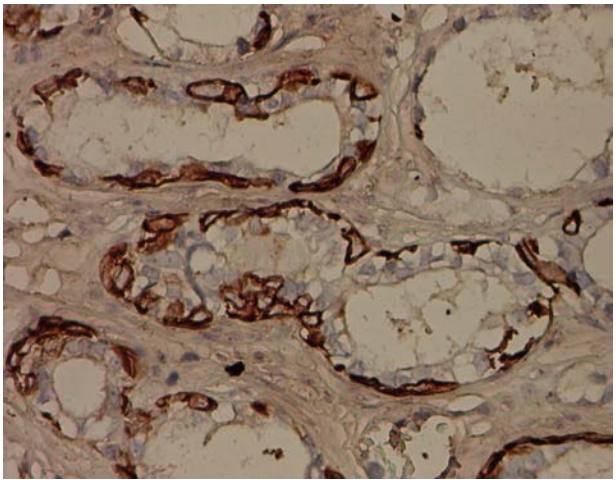

Fig. 165 Sclerosing adenosis– positive immunostaining to SMA, x200 (original)

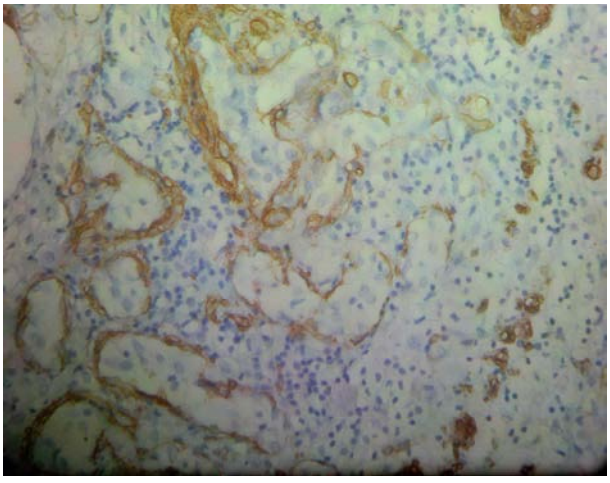

Fig. 167Sclerosing adenosis– positive immunostaining to SMA, x200 (original)

Results and discussion of parameters evaluated between adenocarcinomas with small glands and atrophy

Between 2008-2011, there was a number of 19 cases of prostatic atrophy, with an incidence of 1.04%. The value obtained in my study is lower than that found by other authors, 85% at autopsy [15] and 83.7% on biopsy [16]. In the study group, the lesion was diagnosed in patients aged between 56 and 87 years. We found an association with benign nodular hyperplasia (in 9 cases), according to the literature.

Regarding diameter foci examined, the results were statistically significant ($p < 0.05$). They measured on average 2 mm, with a standard deviation of 0.91.

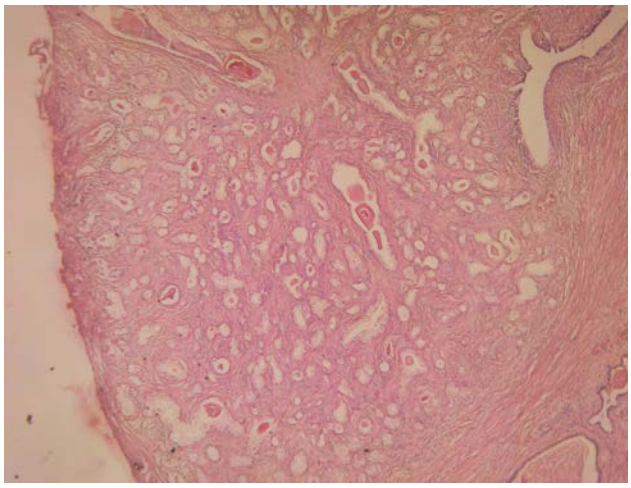

Fig. 172 Lobular atrophy - central duct, H&Ex40, (original)

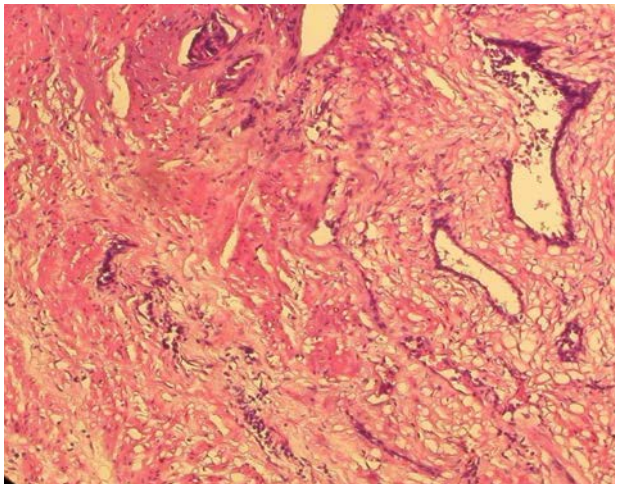

Fig. 176 Linear atrophy - basophilic glands appearance, H&Ex100, (original)

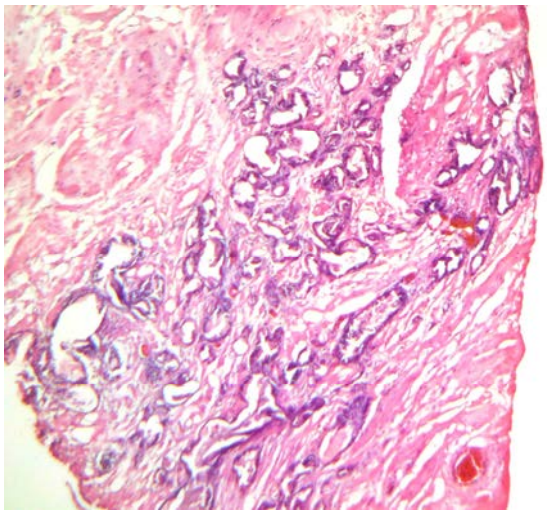

Fig. 179 Lobular atrophy (postatrophic hyperplasia) - minimum and marked distance between glands, H&Ex40 (original)

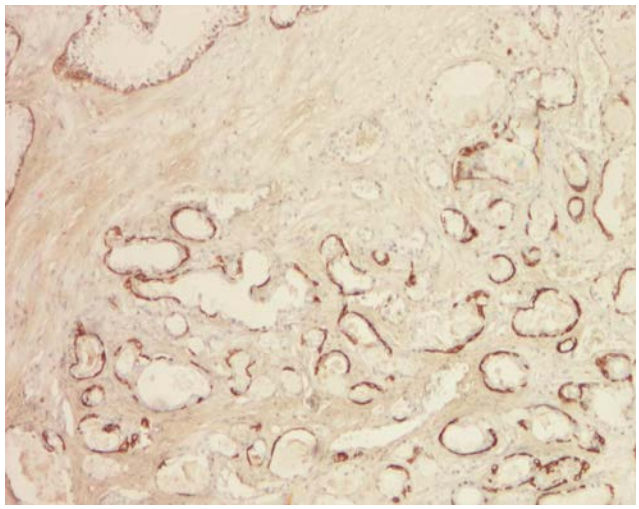

Fig. 189 Atrophy-34βE12 positive discontinuous in basal cells, x40 (original)

Also assessing the number of glands was statistically significant for both types of lesions. This result was due to the greater number of cases of atrophic glands consisting of 10-30 (84.21%), while the number of cases with 30-50 glands is very low (15.78%).

We identified a lobulated appearance of the lesion in 84.21% of atrophy cases, while in 86.95% of adenocarcinomas was absent. However, in 3 cases of atrophy this was absent. This may be due to the fact that group of atrophy consists of multiple histological types: simple (lobular), cystic sclerosing, linear, and some of these is characterized by lobular appearance. There are occasions when it is necessary to differentiate atrophy by adenocarcinoma with atrophic pattern.

Regarding the existence of a the central duct-like structures, the results were statistically significant ($p < 0.05$).

In 36.84% of cases were identified corpus atrophy amilacei, while in 63.15% content was absent.

Evaluation of basal cells with high molecular weight citokeratins (clone 34βE12) revealed the absence of basal cells in all cases of adenocarcinoma, while continuously (78.95%) and discontinuous (21.05%) imunoreaction was positive in cases of atrophy, which emphasized the integrity of the cell layer.

Results and discussion of parameters evaluated between adenocarcinomas with small glands and Cowper glands

Cowper glands, known as bulbourethral glands are periurethral pair yellow structures, located in the urogenital diaphragm, near the prostatic apex.

Cowper glands may be confused with well-differentiated adenocarcinoma due to architectural aspect, represented by small glands, crowded, back to back arranged.

Table no. LII Comparison between architectural parameters of AS and ADK with small glands

Parameter	Evaluation criteria	Number of ADK cases	Number of Cowper glands cases	Test	p
Focus diameter	-	3,34±2,34	1,6±0,46	t-test	p<0,05
Number of glands	10-30	0	0	t-test	p<0,05
	30-50	56	5		
	>50	13	5		
Lobular pattern	Absent	60	0	$\chi 2$	p<0,05
	Present	9	10		
Central duct	Absent	69	3	$\chi 2$	p<0,05
	Present	0	7		
Pleomorphism of the	Absent	19	3	$\chi 2$	p>0,05

glands	Slight	23	3		
	Marked	27	4		
	Absent	40	5	$\chi 2$	p>0,05
	Minimum (1-3 celule)	29	4		
	Marked (more than 3 cells)	0	1		
Periglandular eosinophilic halo	Present	0	0	$\chi 2$	p>0,05
	Absent	69	10		

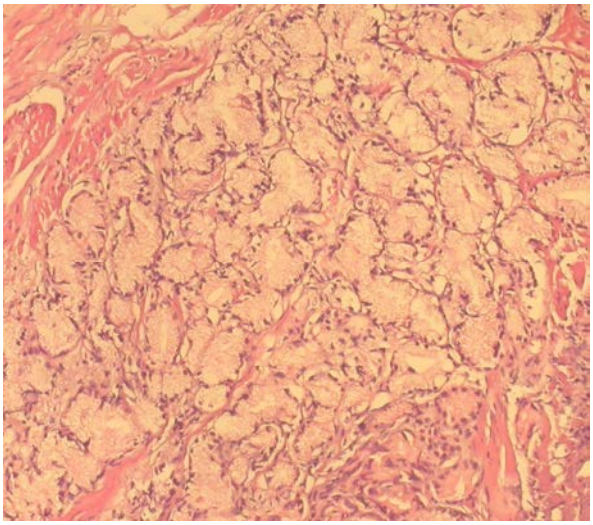

Fig. 194 Cowper glands - slightly glandular pleomorphism, H&Ex200, (original)

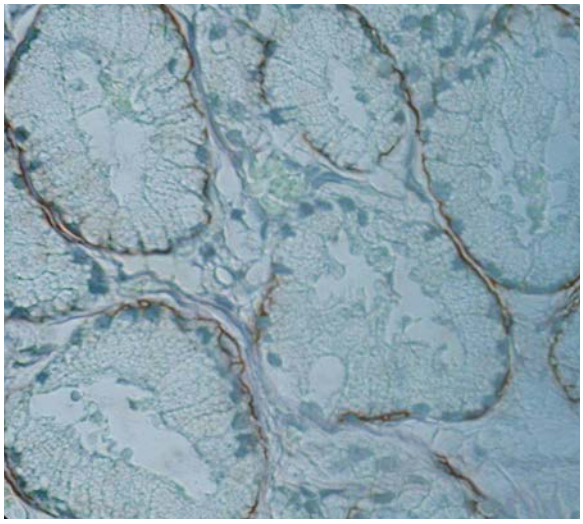

Fig.195 Cowper glands– presence of basal cell layer, 34βE12 x200, (original)

Regarding the existence of a central duct-like structures, the results were statistically significant ($p < 0.05$). We identified corpora amilacei in 20% of cases of Cowper glands, compared with 2.89% of adenocarcinomas. Cristaloids were present mainly in adenocarcinomas (75.36%), and they were absent in Cower glands. The results were statistically significant ($p < 0.05$). Basal cells were present continuously at Cowper glands, as evidenced by positive imunostaining in all cases. Cases studied were negative for PSA, like other studies [17,18,19].

Results and discussion of parameters evaluated between adenocarcinomas with small glands and basal cell hyperplasia

Basal cell hyperplasia was associated with benign prostatic hyperplasia at a rate of 57.14% (12 cases). This combination is similar to the literature data, that the lesion is diagnosed as nodular hyperplasia component. HCB may be complete or incomplete.

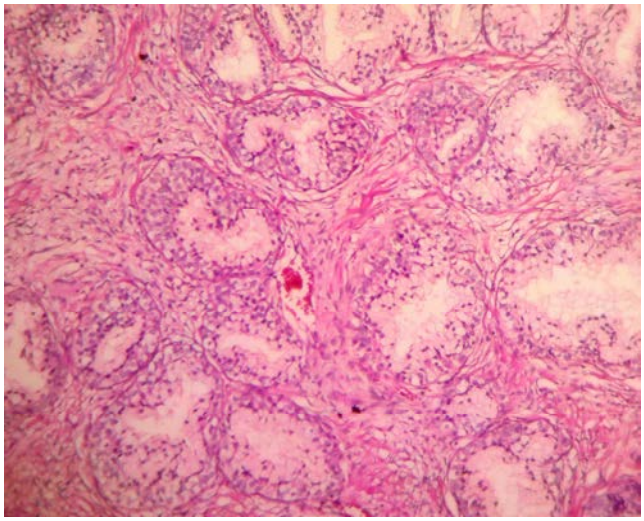

Fig. 198 Incomplete basal cell hyperplasia, nodular appearance, H&Ex100, (original)

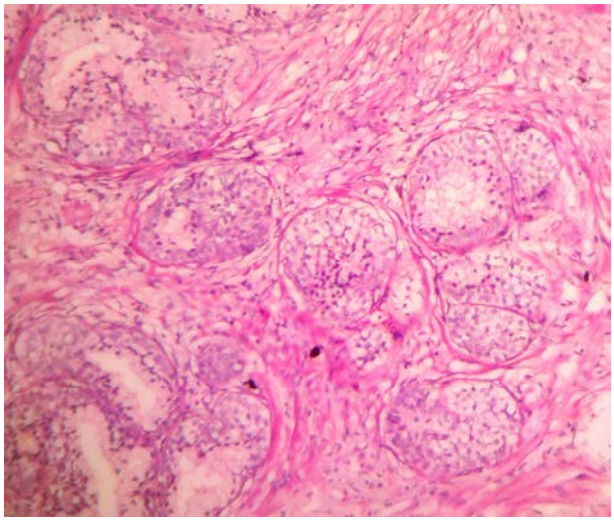

Fig. 199 Complete and incomplete basal cell hyperplasia, H&Ex100, (original)

Most often incomplete form of basal cell hyperplasia may be confused with adenocarcinoma, due to the microacinar appearance and minimum proliferation of basal cell layer. Unlike all other lesions that mimic adenocarcinoma, we found that most foci (95.23%) were composed of less than 10 glands, and one case was represented by 10-30 glands. We have not identified cases of HCB consisting of more than 30 glands. The results were statistically significant ($p < 0.05$).

Lobulated appearance was found in 80.95% of cases of HCB, while 86.95% of adenocarcinomas was absent. The results were statistically significant ($p < 0.05$). Regarding immunohistochemical study, all 21 cases of BCH showed continuous positive imunostaining for 34βE12 of basal cells.

Results and discussion of basaloid carcinoma

Another extremely rare lesion that caused issues of differential diagnosis of prostate was basaloid carcinoma. Between 2008-2011, we identified one case, recorded a rate of 0.05%. On microscopic exam, we observed proliferation of nests composed by neoplastic basophilic and basaloid cells with round-oval shape. The nuclei were large with atypia.

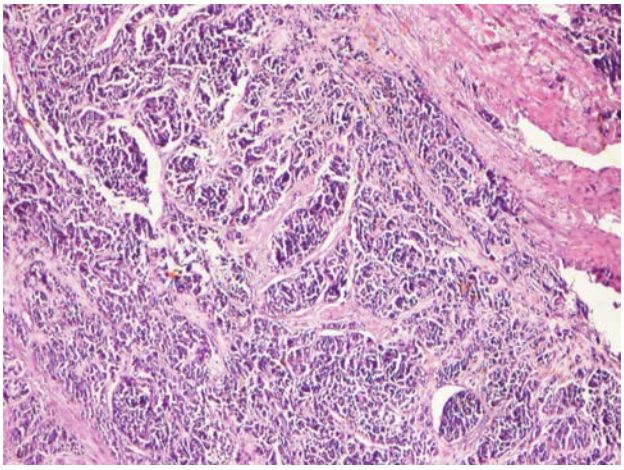

Fig.207 Bazaloid carcinoma, H&Ex100, (original)

Immunohistochemical techniques showed an intense positivity for Ki67 compared with typical and atypical HCB.

Comparative assessment of lesions including large glands

The most common lesion that mimics large gland adenocarcinomas (Gleason grade 3, 4 and 5 cribriforme comedonecroză) is clear cell cribriform hyperplasia (HCCC). The four cases of HCCC had nodular architecture and were composed of 3-6 glands papillary-cribriform appearance. Nuclei were characterized by round-oval shape without mitosis, showing characteristic phenomenon of aging. The lumen of these lesions showed no specific content, except for one case which contained rare amilacei corpora. This feature was not similar to the literature data, according to which the lumen may contain crystalloids, mucin, glycogen. In addition, all cases were associated with nodular benign prostatic hyperplasia.

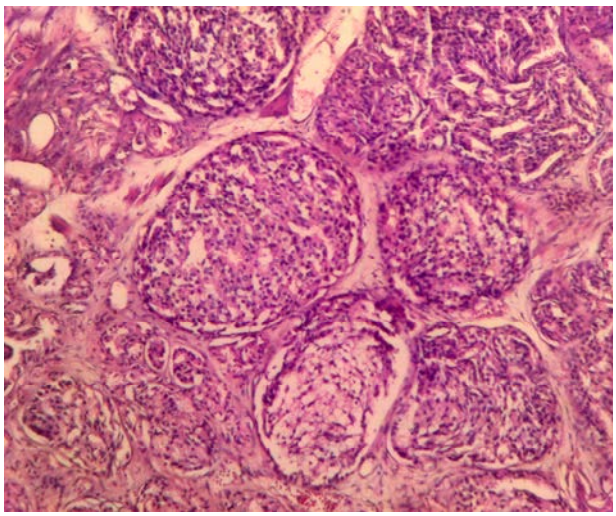

Fig. 212 Cribriform adenocarcinoma, Gleason grade 3– H&Ex40, (original)

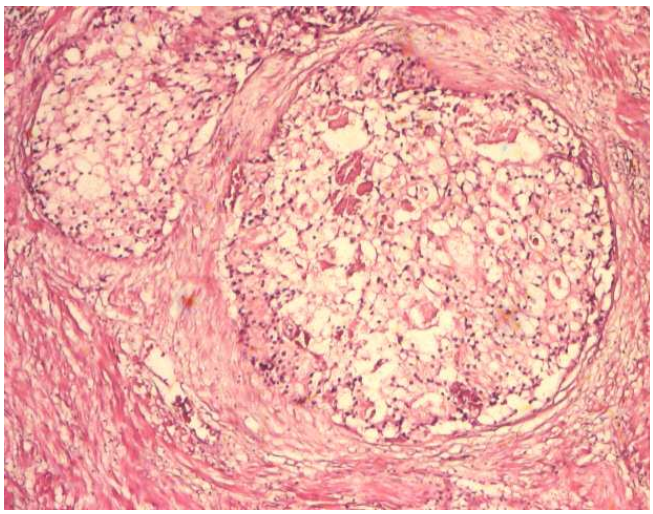

Fig. 211 Clear cell cribriform hyperplasia– circumscribed appearance and rare intraluminal corpora amilacei,H&Ex40, (original)

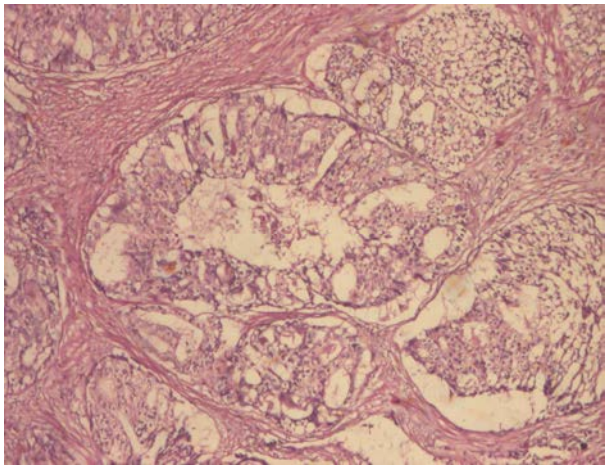

Fig. 215 Adenocarcinoma with comedonecrosis, Gleason grade 5, H&Ex100, (original)

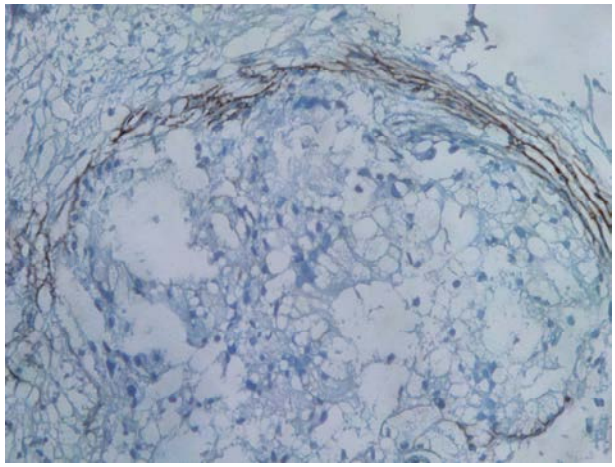

Fig. 221 Clear cell cribriform hyperplasia, presence of basal cell, 34βE12x200, (original)

Application of monoclonal antibodies revealed continuously (two cases) and discontinuous (two cases) positive imunostaining to 34βE12 in HCCC cases and negative staining in adenocarcinomas.

Comparative assessment of fused glands lesions

This architecture is found in adenocarcinomas with fused glands (Gleason grade 4) and xantogranulomatous inflammation. Xantogranulomatous inflammation is an uncommon inflammatory process of the prostate, which can mimic both clinically and histologically an adenocarcinoma with Gleason grade 4. Collections of foamy macrophages may create problems of differential diagnosis with the variant of adenocarcinoma called by Gleason hipernephromatoid (due to similarity with clear cell carcinoma ofthe kidney), previously classified 4B.

Between 2008-2011 were identified seven cases of prostatic xantogranulomatous inflammation.

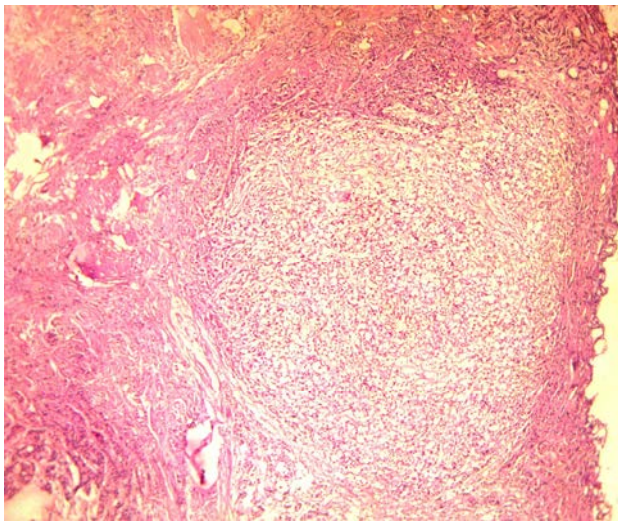

Fig. 225 Fused glands adenocarcinoma, Gleason grade 4, H&Ex40 (original)

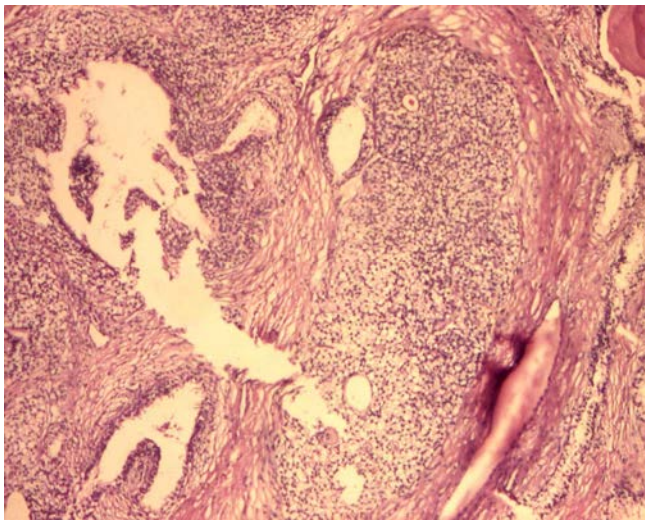

Fig.227 Xantogranulomatous Inflammation around some discontinuous ducts , H&Ex40 (original)

Differential diagnostic problems arising from the fact that some adenocarcinomas has no nuclear changes typical of malignancy and characterized by small hyperchrome nuclei without prominent nucleoli. The application of CD68 antibodies showed positive imunostaining of foamy macrophages. In case of Gleason 4 adenocarcinoma, the reaction was negative.
PSA was positively to prostatic epithelial cells and negative in the nodular collections of histiocytes.

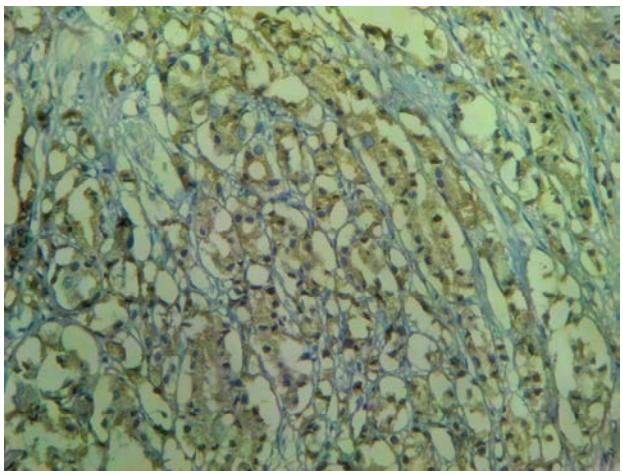

Fig. 235 Adenocarcinom Gleason grade 4, PSA positive, x100 (original)

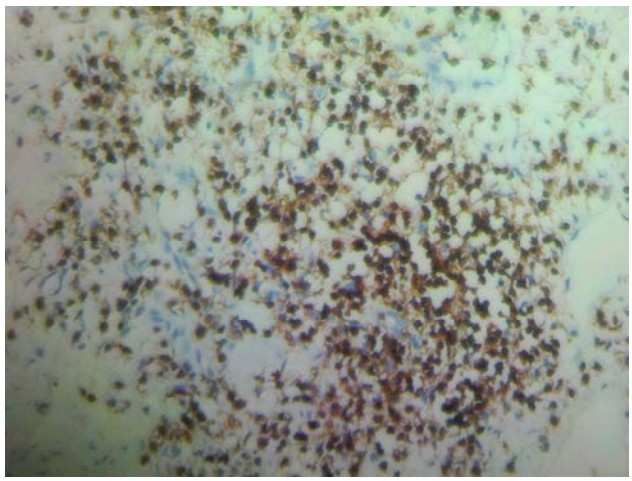

Fig. 233 Xantogranulomatous inflammation, CD 68 positive, x200 (original)

Comparative assessment of lesions with solid architecture

Comparative assessment of solid adenocarcinomas and nonspecific granulomatous inflammation of the prostate

In this category of Gleason grade 5 adenocarcinomas cells have the appearance of islands or isolated or solid cords. Lesions that simulate this architecture are inflammatory lesions. Between 2008-2011 were diagnosed seven cases of nonspecific granulomatous inflammation, with a frequency of 0.38%. The results are quite similar to those published in Stillwell's study, which found a rate of 0.5% [20]. Microscopically, adjacent to the lesions descibed, we noted the presence of nodular or diffuse collections of macrophages, lymphocytes, plasma cells, epithelioid cells and rarely giant cells.
In order to distinguish adenocarcinoma by nonspecific granulomatous prostatitis I used prostatic epithelial (PSA) and limphohistiocytes (CD68) markers.

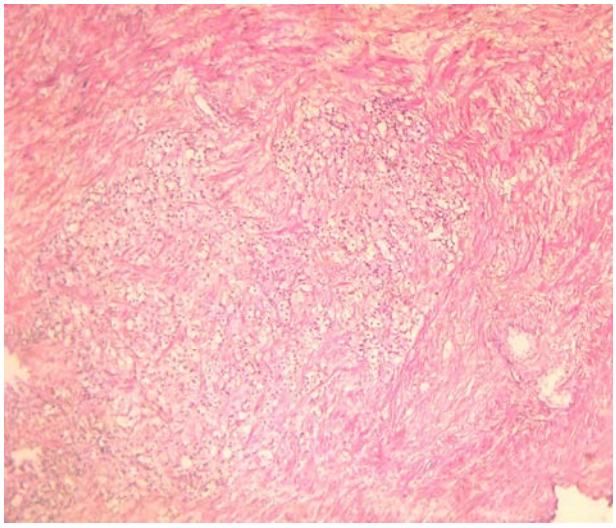

Fig. 239 Nonspecific granulomatous inflammation, H&E x40, (original)

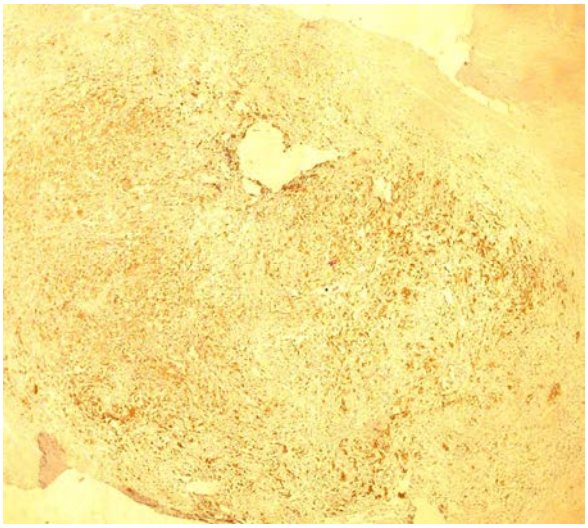

Fig. 244 Nonspecific granulomatous inflammation, CD 68 pozitiv, x100, (original)

Comparative assessment of solid adenocarcinomas and nonspecific chronic inflammation of the prostate

The study group consisted of 42 cases of nonspecific chronic inflammation, with a frequency of 2.3%. PSA ranged between 4 and 27 ng / ml. On microscopic examination preparations, I found the presence of an inflammatory infiltrate with the nodular or diffuse available with either periglandulară available either on the stroma, variable intensity. This infiltrate was composed of lymphocytes and plasma cells. Nonspecific chronic inflammation were simulated a undifferentiated adenocarcinoma, especially in situations when the associated artifacts caused by fixation or processing of the fragments, when they were associated with atrophic changes of high intensity. In difficult cases, immunohistochemical techniques using both prostatic epithelial markers (PSA - positive adenocarcinomas) and leukocyte (CD45 - positive inflammation) established diagnosis.

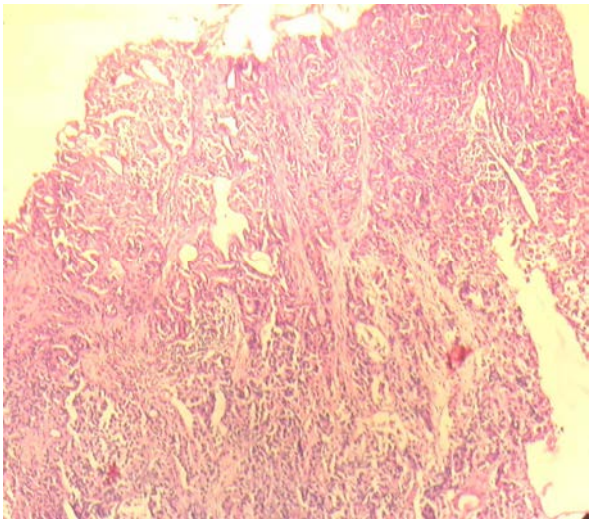

Fig. 249 Adenocarcinoma, Gleason grade 5, H&Ex100, (original)

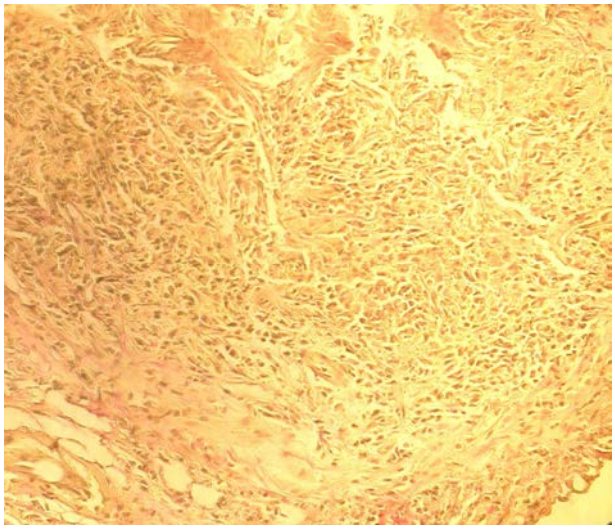

Fig.251 Nonspecific chronic inflammation which simulates a solid adenocarcinoma, van Giesonx100, (original)

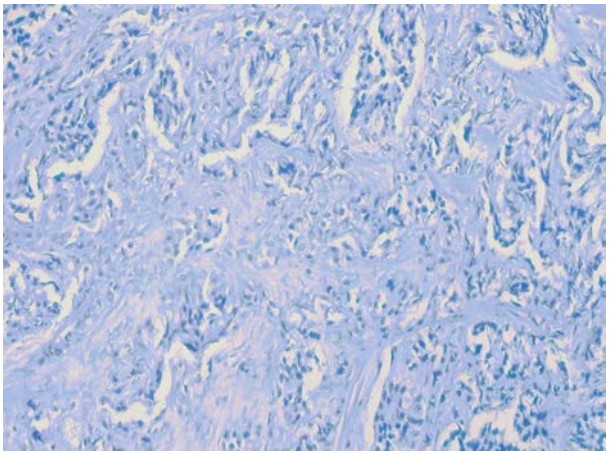

Fig. 255 Nonspecific chronic inflammation with artefactuale retraction, PSA negative immunoreaction, x40, (original)

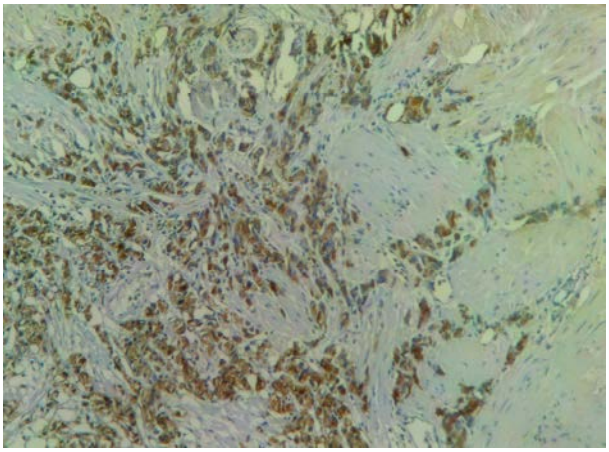

Fig. 256 Adenocarcinoma Gleason grade 5, PSA positive immunoreaction, x40, (original)

Assessment of inflammatory pseudotumour of the prostate case

By studying casuistry between 2008-2011, we identified one case diagnosed with inflammatory pseudotumour (miofibroblastic inflammatory tumor). Histologically, the lesion was represented by a spindle cell proliferation in a loose stroma with multiple small vessels with similar appearance of granulation tissue. Throughout the proliferation, we identified a moderate chronic inflammatory infiltrate.

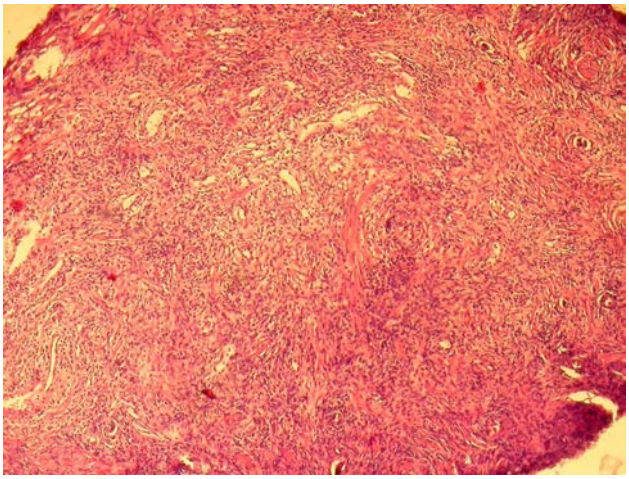

Fig. 259 Inflammatory pseudotumor, spindle cell appearence,H&Ex40, (original)

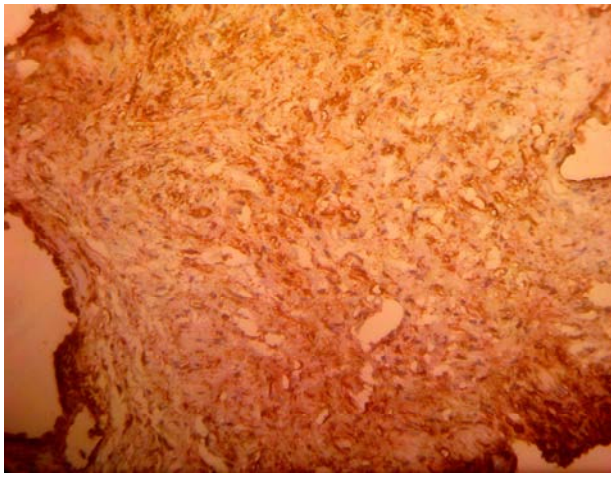

Fig. 261 Inflammatory pseudotumor positive to Vimentin, x100 (original)

X. Morphometric evaluation of adenocarcinoma and lesions that mimic malignancy

The number of morphometric studies of the different structural components of human prostate is reduced on international level. Nuclear morphometry is a method mainly for laborious research, and although has a role in assessing the progression of the neoplastic process, is not fully known its clinical utility. In this respect, there is still no consensus regarding defaults prostatic lesions reference, so it is considered an important area of research.

X.1. Morphometric evaluation of the control group

To assess nuclear changes of prostatic epithelial component, we used a semiautomatic technique. The control group was represented by 30 cases diagnosed with benign prostatic hyperplasia.

Table no. LXIV Nuclear morphometric values of control group

Nuclear values	AN (μm^2)	Deq (μm)	Dmax (μm)	Dmin (μm)	E	P (μm)
minimum value	35,83	6,75	7.55	4,81	1,1	20,22
maximum value	56,64	8,63	11.67	8,24	1,78	27,84
mean value	49,38	7,91	9,32	6,74	1,32	24,02
standard deviation	5,7	0,47	0,87	0,81	0,16	1,71

Although we have not measured the normal tissue nuclei, this suggests that hormonal stimulus resulting benign gland hyperplasia, without cyto-nuclear changes. This hyperplasia results in organ hypertrophy.

Studies are controversial in terms of histological elements with the direct role in prostate hyperplasia. The main theories refer either to epithelial component, according to studies by Price 1990 and Eri 2000 [21.22] or the stromal component as Chagas Barstch 1979 and 2002 [23.24], the latter being accepted with predilection. The mean value of nuclear area in controls are similar to the results obtained by Wang et al in 1992 on normal prostate tissue, whose mean values were 54.2 ± 3.1 μm [25].

Calculating the Pearson correlation coefficient (MedCalc version 12.2.1.0, trial) between morphometric parameters show that there is a strong correlation between:

- AN and P ($r = 0.8560$, $p < 0.0001$),
- AN and Deq ($r = 0.9994$, $p < 0.0001$),
- AN and Dmax ($r = 0.5882$, $p = 0.0006$),
- AN and Dmin ($r = 0.6498$, $p = 0.0001$).

The only parameter which does not correlates with the nuclear area is elongation factor E, which has a weak negative correlation type ($r = -0.2364$) but not statistically significant ($p = 0.2364$).

X.2. Morphometric evaluation of architecture represented by small glands

• Morphometric evaluation of small gland adenocarcinomas

Following measurements, we obtained the following values of nuclear parameters:

Table no. LXV Nuclear morphometric values in small glands adenocarcinomas

Nuclear values in adenocarcinomas	AN (µm²)	Deq (µm)	Dmax (µm)	Dmin (µm)	E	P (µm)
minimum value	49,88	7,97	8,24	6,71	1,06	24,27
maximum value	138,48	13,23	15,31	11,54	1,57	41,6
mean value	70,46	9,38	10,98	8,16	1,38	28,97
standard deviation	16,85	1,06	1,34	0,98	0,12	3,33

In prostatic adenocarcinomas with the small glands, nuclei ranged from similar size to benign lesions to those hyperchromatic characterised by increase volume.

Tabel nr. LXVI Comparison between morphometric parameters determined in the control group and small glands adenocarcinomas

morphometric parameter	**Lesion**		**t-test**
	Controls	Small glands ADK	P value
nuclear area mean value (µm²)	49,38	70,46	p=0,0001
mean diameter average value (µm)	7,91	9,38	p<0,0001
Maximus diameter average value (µm)	9,32	10,98	p<0,0001
Minimum diameter average value (µm)	6,74	8,16	p<0,0001
Elongation mean value	1,32	1,38	p=0,0379
Perimeter mean value (µm)	24,02	28,97	p<0,0001

Nuclear morphometry is useful in differentiating benign prostatic hyperplasia from adenocarcinomas, similar to that observed in the study of Taboga et al. in 2003 [26]. Still there is no consensus regarding standard values for the parameters evaluated nuclear prostatic lesions. Published data variability can be explained by the fact that histologically prostate cancer is a heterogeneous organ and studies compared different regions with distinct morphological features [27]. After determining the correlations between parameters evaluated in small gland adenocarcinomas, we found that there is a strong correlation, except elongation ($r = 0.09370$, $p = 0.4438$).

My results are similar to those found by Wang in 1992.

Morphometric evaluation of atypical adenomatous hyperplasia cases (HAA)

It was assessed a total of 60 cases of HAA. Measurements in the nuclei of epithelial cells revealed values that are summarized in the next table:

Table no. LXVII Morphometric values of epithelial cell nuclei in HAA

Nuclear values in HAA	AN (μm^2)	Deq (μm)	Dmax (μm)	Dmin (μm)	E	P (μm)
minimum value	38,19	6,97	7,55	6,18	1,22	21,6
maximum value	85,34	10,42	11,67	8,93	1,31	31,46
mean value	58,11	8,55	10,14	7,3	1,37	26,31
standard deviation	9,99	0,71	1,06	0,65	0,11	2,31

Calculating the Pearson correlation coefficient between morphometric parameters showed a strong correlation between:

- AN and P (r=0,9784, p<0,0001),
- AN and Deq (r=0,9978, p<0,0001),
- AN and Dmax (r=0,8772, p<0,0001),
- AN and Dmin (r=0,8586, p<0,0001).

Between nuclear area and elongation have not been determined correlation (r = 0.2390, p = 0.0659).

Tabel nr. LXVIII Comparison of nuclear morphometric parameters of control group / HAA

morphometric parameter	**Lesion**		**t-test**
	Controls	HAA	P value
Nuclear area mean value (μm^2)	49,38	58,11	p<0,0001
Mean diameter average value (μm)	7,91	8,55	p<0,0001
Maximus diameter average value (μm)	9,32	10,14	p=0,0004
Minimum diameter average value (μm)	6,74	7,3	p=0,0007
Elongation mean value	1,32	1,37	p=0,0551
Perimeter mean value (μm)	24,02	26,31	p<0,0001

By comparing the nuclear parameters between cases of HAA group with the control group, the results were statistically significant for nuclear area, mean diameter, minimum and maximum ($p < 0.05$), except elongation ($p > 0.05$).

Tabel nr. LXIX Comparison of nuclear morphometric parameters of adenocarcinomas with small glands / HAA

morphometric parameter	**Lezion**		**t-test**
	HAA	Small glands ADK	P value
nuclear area mean value (μm^2)	58,11	70,46	p<0,0001
mean diameter average value (μm)	8,55	9,38	p<0,0001
Maximus diameter average value (μm)	10,14	10,98	p=0,0002
Minimum diameter average value (μm)	7,3	8,16	p<0,0001
Elongation mean value	1,37	1,38	p=0,7731
Perimeter mean value (μm)	26,31	28,97	p<0,0001

Between cases of HAA and small glands adenocarcinoma results were statistically significant for nuclear area, mean diameter, minimum and maximum ($p < 0.05$), except elongation ($p > 0.05$). Morphometric characteristics of HAA are intermediate between the ADK and the control group represented by BPH, indicating a possible preneoplastic potential.

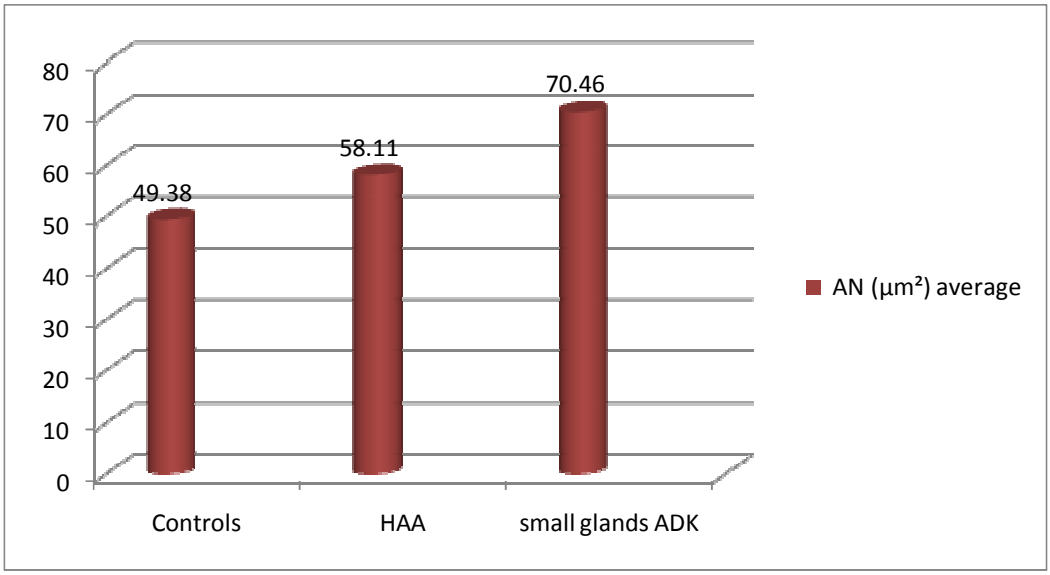

Fig. Nr. 269 Comparative representation of nuclear areas in small glands adenocarcinomas, HAA and benign prostatic hyperplasia

Morphometric evaluation of cases diagnosed with sclerosing adenosis

The assessment of nuclear component of glandular epithelial cell of 33 cases of sclerosing adenosis, we obtained values systematized in the table below:

Tabel nr. LXX Morphometric nuclear values of epithelial cells in AS

Nuclear values in AS	AN (µm²)	Deq (µm)	Dmax (µm)	Dmin (µm)	E	P (µm)
minimum value	32,14	6,4	7,61	5,7	1,33	18,97
maximum value	69,5	8,79	10,14	7,61	1,31	26,8
mean value	48,39	7,78	9,06	6,81	1,31	23,83
standard deviation	9,23	0,71	0,94	0,7	0,11	2,38

Calculating the Pearson correlation coefficient showed a strong correlation between: AN and P ($r=0,9383$, $p<0,0001$), AN and Deq ($r=0,9848$,$p<0,0001$), AN and Dmax ($r=0,8489$, $p<0,0001$), AN and Dmin ($r=0,7375$, $p<0,0001$). The only factor that was not correlated with nuclear area was elangation ($r = 0.07236$, $p = 0.6890$).

Table no. LXXI Comparison of nuclear parameters between cases of sclerosing adenosis/control group

morphometric parameter	Lesion		t-test
	Controls	AS	Valoarea p
nuclear area mean value (µm²)	49,38	48,39	p=0,6145
mean diameter average value (µm)	7,91	7,78	p=0,4229
Maximus diameter average value (µm)	9,32	9,06	p=0,2593
Minimum diameter average value (µm)	6,74	6,81	p=0,7223
Elongation mean value	1,32	1,31	p=0,8467
Perimeter mean value (µm)	24,02	23,83	p=0,7084

Following the application of t-test, we found that between the parameters evaluated in sclerosing adenosis and control group, the differences were not statistically significant. Thus, sclerosing adenosis parameters have values similar to those of benign prostatic hyperplasia. Between nuclear parameters of sclerosing adenosis and small glands adenocarcinoma the differences were statistically significant ($p < 0.05$).

Morphometric evaluation of prostatic atrophy cases

Nuclear morphometric measurements were performed on a sample of 19 cases of atrophy.

Table no. LXXIII Morphometric nuclear values of epithelial cells in prostatic atrophy

Nuclear values in atrophy	AN (µm²)	Deq (µm)	Dmax (µm)	Dmin (µm)	E	P (µm)
Minimum value	43,38	7,43	8,24	5,26	1,2	23,19
Maximum value	65,54	9,09	13,05	8,16	1,69	29,13
Mean value	54,02	8,25	10,26	6,82	1,41	25,84
Standard deviation	6,42	0,48	1,21	0,6	0,13	1,74

Calculating the Pearson correlation coefficient of prostatic atrophic lesions showed a strong correlation between nuclear parameters, except elongation (r= -0,04802 p=0,8452).

Table no. LXXIV Morphometric nuclear values of epithelial cells in small glands adenocarcinoma/atrophy

morphometric parameter	Lesion		t-test
	small glands adenocarcinoma	Atrophy	P value
Nuclear area mean value (µm²)	70,46	54,02	p=0,0001
Mean diameter average value (µm)	9,38	8,25	p<0,0001
Maximus diameter average value (µm)	10,98	10,26	p=0,0384
Minimum diameter average value (µm)	8,16	6,82	p<0,0001
Elongation mean value	1,38	1,41	p=0,2965
Perimeter mean value (µm)	28,97	25,84	p=0,0002

The results were statistically significant for nuclear area, perimeter, average diameter, minimum and maximum ($p < 0.05$). They have not been significant for elongation ($p > 0.05$). Between nuclear parameters of atrophy and the control group, the differences were statistically significant ($p < 0.05$), except the minimum diameter. We found that the parameters of atrophy are higher than those of benign hyperplasia.

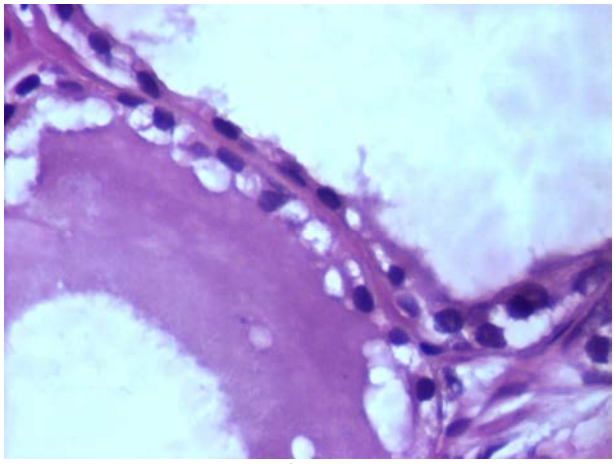

Fig. 273 The nuclear features in cystic atrophy, H&Ex400, (original)

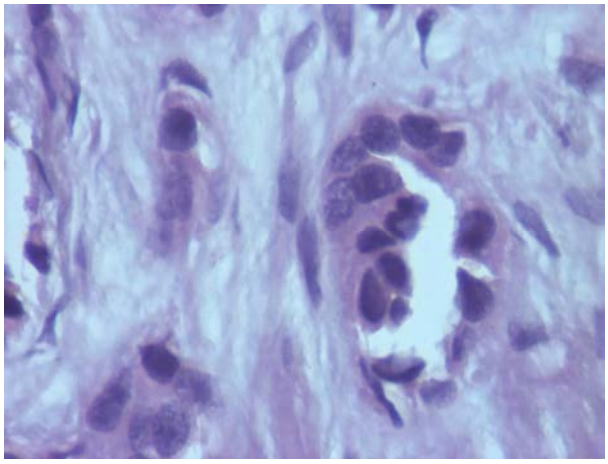

Fig. 275 Large and hyperchrome nuclei in atrophic adenocarcinoma, H&Ex400, (original)

Morphometric evaluation of Cowper glands

We assessed a number of 10 cases of Cowper glands, which have been identified in prostate tissue adjacent to benign prostatic hyperplasia changes.
The values found are summarized in the table below:

Table no. LXXVI Average values of the nuclear parameters of epithelial cell nuclei in Cowper glands

Nuclear values of HCB	AN (µm²)	Deq (µm)	Dmax (µm)	Dmin (µm)	E	P (µm)
minimum value	49,51	7,94	8,93	6,87	1,18	23,83
maximum value	63,08	8,94	10,51	8,32	1,5	27,53
mean value	56,28	8,45	9,88	7,44	1,33	26,02
standard deviation	4,36	0,34	0,58	0,4	0,12	1,19

Calculating the Pearson correlation coefficient between the parameters describing the Cowper glands, revealed a strong correlation, except Dmin ($r = 0.1993$, $p = 0.5809$) and elongation ($r = 0.4626$, $p = 0, 1782$).
Calculating the Pearson correlation coefficient between the parameters describing the nuclei of Cowper glands revealed a strong correlation, except Dmin ($r = 0.1993$, $p = 0.5809$) and elongation ($r = 0.4626$, $p = 0, 1782$).

Morphometric evaluation of of cases of basal cell hyperplasia

In order to calculate nuclear morphometric parameters has been assessed a number of 21 cases of HCB. The nuclei were measured in both cases of complete and incomplete basal cells hyperplasia. The data were systematized in the table:

Table no. LXXIX Morphometric nuclear values of HCB

Nuclear values in HCB	AN (µm²)	Deq (µm)	Dmax (µm)	Dmin (µm)	E	P (µm)
minimum value	48,57	7,86	9,61	5,49	1,07	24,68
maximum value	98,07	9,53	12,44	9,57	1,88	36,15
mean value	74,48	9,67	11,59	8,24	1,43	30,23
standard deviation	14,57	0,96	1,21	1,25	0,24	3,01

The Pearson correlation coefficient determination, revealed a strong correlation between all parameters evaluated: AN and P (r = 0.9853, p <0.0001), NA and DEQ (r = 0.7728, p <0.0001), NA and Dmax (r = 0.7543, p = 0.0001), NA and Dmin (r = 0.7946, p <0.0001), NA elongation (r = 0.9785, p <0, 0001).
The comparative evaluation of the mean values of nuclear parameters between the control group and HCB have been noticed that the results are statistically significant (p <0.05).

Tabel nr. LXXXI Comparison of nuclear parameters between basal cell hyperplasia and small glands adenocarcinoma

morphometric parameter	**Leziune**		**t-test**
	Small glands ADK	HCB	Valoarea p
Nuclear area mean value (µm²)	70,46	74,48	p=0,3266
Mean diameter average value (µm)	9,38	9,67	p=0,2736
Maximus diameter average value (µm)	10,98	11,59	p=0,0647
Minimum diameter average value (µm)	8,16	8,24	p=0,7743
Elongation mean value	1,38	1,43	p=0,2382
Perimeter mean value (µm)	28,97	30,23	p=0,1254

Between HCB and small glands adenocarcinomas, we have not identified statistically significant differences (p> 0.05).

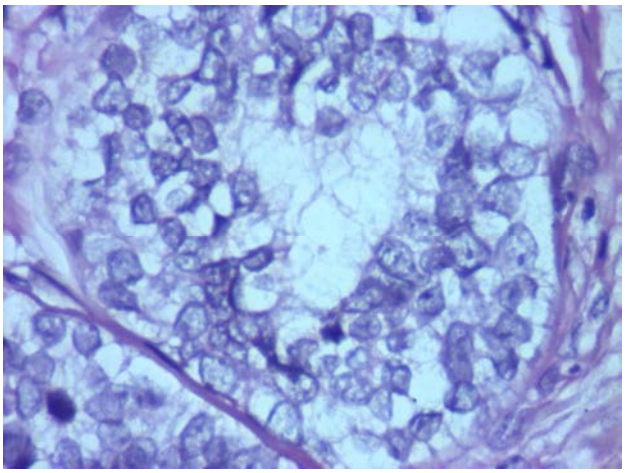

Fig. 278 Nucear features in incomplete HCB, H&Ex400, (original)

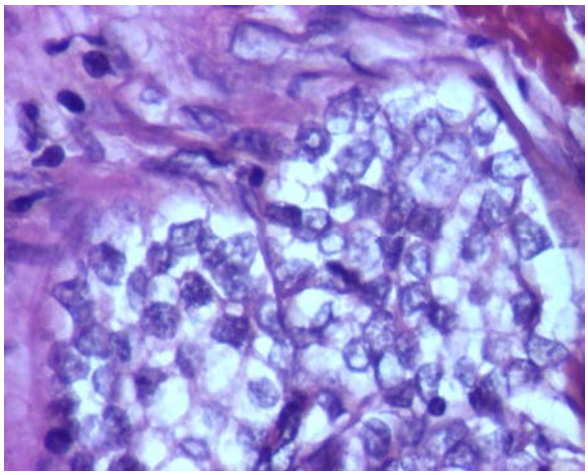

Fig. 279 Nucear features in complete HCB, H&Ex400, (original)

My measurement values were different from those obtained by Montironi et al in 2005 which showed that nuclear area increased from 27.95 μm ² for basal cell hyperplasia to 38, 61 μm ² for florid HCB, reaching a maximum of 53 , 52 μm ² for basaloid carcinoma [28].

Morphometric assessment bazaloid prostate carcinoma case

After studying the casuistry of prostate tumors in Clinical Pathology Department between 2008-2011, we identified one case of carcinoma bazaloid. This is a rare variant of prostatic carcinoma.

Table no. LXXXII Morphometric values of nuclear basaloid prostate carcinoma

Nuclear values in basaloid carcinoma	AN (μm²)	Deq (μm)	Dmax (μm)	Dmin (μm)	E	P (μm)
Average	97,41	11,09	13,27	9,45	1,41	34,71

In the case of basaloid carcinoma, nuclear area did not correlate with other parameters ($p > 0.05$). Nuclear parameters of basaloid carcinoma is characterized by higher values of parameters compared in basal cell hyperplasia and adenocarcinoma in small glands.

X.3. Morphometric evaluation of architecture represented by large glands

Morphometric evaluation of large glands arhitecture

In adenocarcinomas with large glands, nuclei were characterized by minimum, maximum and average values of the parameters according to the table below:

Table no. LXXXIII Nuclear parameter values in adenocarcinomas with large glands

Nuclear values in large gland adenocarcinomas	AN (μm²)	Deq (μm)	Dmax (μm)	Dmin (μm)	E	P (μm)
minimum value	78,93	9,98	11,19	8,24	1,1	30,58
maximum value	187,76	13,31	17,51	9,93	1,76	47,86
mean value	130,66	12,77	15,31	10,9	1,4	40,31
standard deviation	27,97	1,4	2,13	2,32	0,16	4,76

Variation of maximum and minimum limits of the nuclear area showed marked nuclear pleomorphism. The results are in acordance with those of Choi in 1999, which found that nuclei are irregular and larger with increasing degree of malignancy based on Gleason score [29].

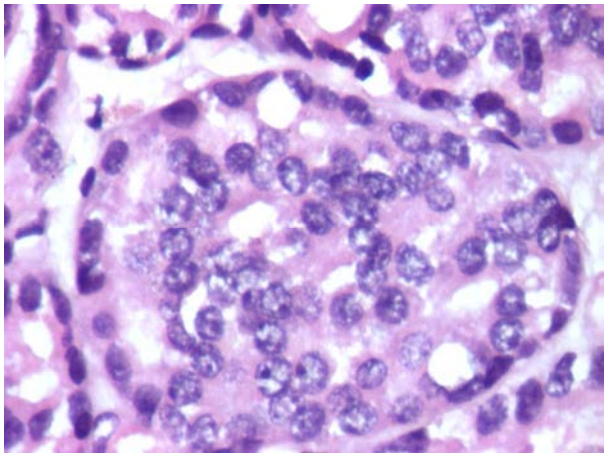

Fig. 283 Large nuclei with visible nucleoli in cribriform adenocarcinoma, H&Ex400, (original)

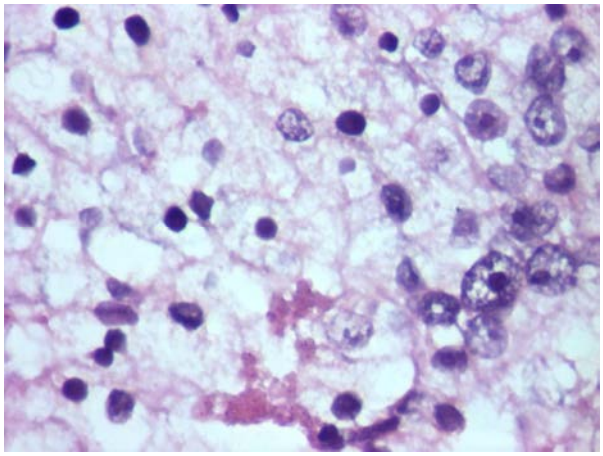

Fig. 284 Nuclear aspects in adenocarcinoma with comedonecrosis, H&Ex400, (original)

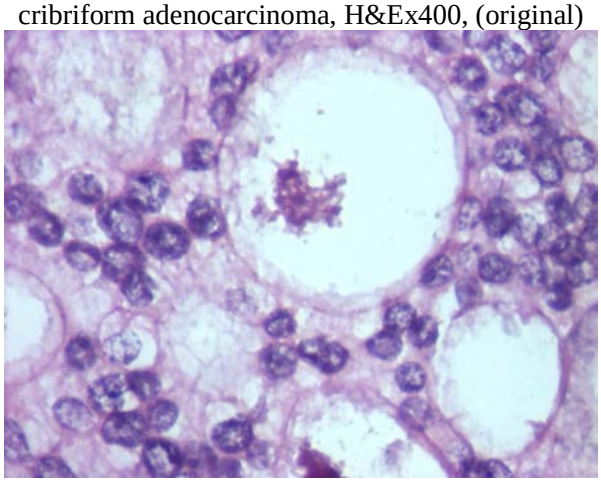

Fig. 285 Visible nucleoli in cribriform adenocarcinoma, H&Ex400, (original)

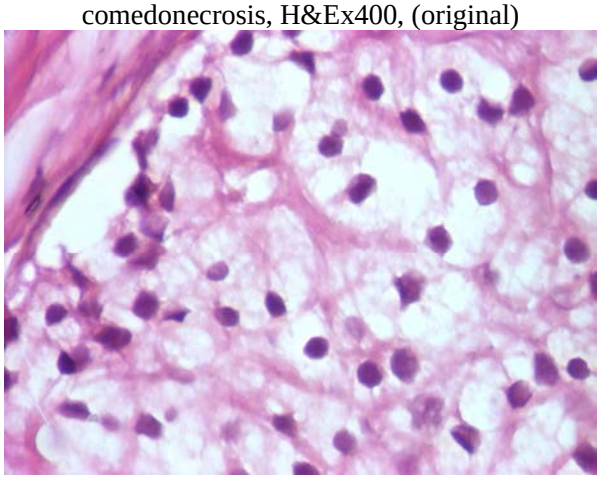

Fig. 286 Small nuclei of clear cell cribriform hyperplasia, H&Ex400, (original)

The Pearson correlation coefficient determination, revealed a strong correlation of the parameters evaluated in large glands adenocarcinoma, between: AN and P (r=0,9431, p<0,0001), AN and Deq (r=0,9970, p<0,0001), AN and Dmax (r=0,7640 p<0,0005). Nuclear area does not correlate with elongation (r = - 0.1649, p = 0.3158) and with Dmin (r = - 0.001712, p = 0.9917).

Also, parameter values are higher than those obtained by small glands adenocarcinomas evaluation. This can be explained by the fact that the augmentation gland leads to increased size of the nuclei.

Morphometric evaluation of cases diagnosed with clear cell cribriform hyperplasia

In clear cell cribriform hyperplasia, nuclei were characterized by minimum, maximum and average values of the parameters according to the table below:

Table no. LXXXV Nuclear parameter values in clear cell cribriform hyperplasia

Nuclear values	AN (µm²)	Deq (µm)	Dmax (µm)	Dmin (µm)	E	P (µm)
Minimum value	55,58	9	9,44	7,47	1,22	25,43
Maximum value	76,86	9,88	1,52	8,73	1,35	30,33
Mean value	71,48	9,46	10,8	8,51	1,27	28,94
Standard deviation	5,26	0,42	0,59	0,25	0,04	1,43

As a result of determining correlations between nuclear parameters evaluated in HCCC we noticed that there is a strong correlation, except for the minimum diameter.

Table no. LXXXVI Nuclear parameters differences between large glands adenocarcinomas and clear cell cribriform hyperplasia

morphometric parameter	**Lesion**		**t-test**
	Large glands adenocarcinomas	HCCC	p value
Nuclear area mean value (µm²)	130,66	71,48	p=0,0001
Mean diameter average value (µm)	12,77	9,46	p<0,0001
Maximus diameter average value (µm)	15,31	10,8	p=0,0002
Minimum diameter average value (µm)	10,9	8,51	p=0,0035
Elongation mean value	1,4	1,27	p=0,1226
Perimeter mean value (µm)	40,31	28,94	p<0,0001

Between nuclear parameters of cases diagnosed with HCCC and large glands adenocarcinomas the differences are statistically significant (p <0.05), except elongation. Between nuclear parameters of HCCC and the control group, the differences are statistically significant (p <0.05), except elongation.

X.4. Morphometric evaluation of architecture represented by fused glands

Morphometric evaluation of fused glands adenocarcinoma

Fused gland adenocarcinomas were characterized by the following values of nuclear parameters determined by semiautomatic morphometry technique:

Table no. LXXXVIII Nuclear parameter values in adenocarcinomas with fused glands

Nuclear values	AN (µm²)	Deq (µm)	Dmax (µm)	Dmin (µm)	E	P (µm)
Minimum value	40,01	7,13	8,49	5,74	1,14	22,05
Maximum value	111,75	11,93	13,48	9,42	1,6	35,54
Mean value	66,82	9,1	10,91	7,79	1,38	28,58
Standard deviation	18,73	1,27	1,7	1,46	0,1	4,22

We found that the value of nuclear area is lower than that obtained in small gland adenocarcinomas and large glands adenocarcinomas. This result is different from the literature data (Choi, 1999).

The Pearson correlation coefficient determination, revealed a strong correlation of the parameters evaluated in fused glands adenocarcinoma between: AN and P (r=0,92 p<0,0001), AN and Deq (r=0,997 p<0,0001), AN and Dmax (r=0,8827 p<0,0001), AN and Dmin (r=0,8441 p<0,0001). The only factor that was not correlated with nuclear area was elangation (r=0,03081 p=0,8649).

Morphometric evaluation of xantogranulomatous inflammations

Xantogranulomatous inflammations were characterized by the following values of nuclear parameters:

Table no. XC The assessment nuclear parameters in xantogranulomatous inflammations

Nuclear values	AN (µm²)	Deq (µm)	Dmax (µm)	Dmin (µm)	E	P (µm)
Minimum value	36,91	6,83	7,65	5,73	1,18	20,34
Maximum value	58,81	8,65	10,19	7,55	1,43	26,91
Mean value	47,34	7,72	8,77	6,93	1,27	23,57
Standard deviation	8,52	0,71	0,83	0,7	0,09	2,39

The Pearson correlation coefficient determination revealed a strong correlation of the parameters evaluated in xantogranulomatous inflammations between: AN and P (r=0,991 p<0,0001), AN and Deq (r=0,9994 p<0,0001), AN and Dmax (r=0,9649 p=0,0004), AN and Dmin (r=0,8982 p=0,006). Elongation does not correlate with nuclear area (r = -0.06339 p = 0.8926).

Table no. XCI Differences between fused glands adenocarcinomas group and xantogranulomatous inflammation

morphometric parameter	**Leziune**		**t-test**
	Fused glands adenocarcinomas	Xantogranulomatous inflammation	p value
Nuclear area mean value (µm²)	66,82	47,34	p=0,0111
Mean diameter average value (µm)	9,1	7,72	p=0,0086
Maximus diameter average value (µm)	10,91	8,77	p=0,0026
Minimum diameter average value (µm)	7,79	6,93	p=0,13
Elongation mean value	1,38	1,27	p=0,0188
Perimeter mean value (µm)	28,58	23,57	p=0,0045

By applying the t-test between adenocarcinomas with fused glands and xantogranulomatous inflammation group, we found that differences between evaluated parameters are statistically significant.

Also, student test showed that between inflammation group and the control group differences are not statistically significant, parameter values obtained being quite close.

X.5. Morphometric assessment of solid architecture

• Morphometric assessment of solid adenocarcinomas

Solid adenocarcinomas showed the following nuclear parameter values:

Table no. Nuclear morphometric parameters in solid adenocarcinomas

Nuclear values	AN (µm²)	Deq (µm)	Dmax (µm)	Dmin (µm)	E	P (µm)
Minimum value	58,97	8,61	10,25	6,18	1,07	26,34
Maximum value	105,62	11,6	9,58	8,24	1,92	38,81
Mean value	72,45	9,55	11,43	8,14	1,43	29,91
Standard deviation	9,97	0,65	1,27	1,09	0,15	2,48

We found that the parameters of solid adenocarcinoma are relatively similar to those obtained in case of small glands adenocarcinoma. The results are different from those obtained in the literature [21].

Following the determining correlations between parameters evaluated in solid adenocarcinomas, I found that there is a strong correlation between: AN and P (r= 0,9547 p<0,0001), AN and Deq (r=0,9973 p<0,0001), AN and Dmax (r=0,7536 p<0,0001), AN and Dmin (r=0,4776 p=0,0076). Elongation does not correlate with nuclear area (r = 0.2147 p = 0.2545).

Morphometric assessment of cases of nonspecific chronic inflammation

Were obtained the following nuclear parameters:

Table no. XCV Nuclear morphometric parameters in chronic nonspecific inflammation

Nuclear values	AN (µm²)	Deq (µm)	Dmax (µm)	Dmin (µm)	E	P (µm)
Minimum value	21,13	5,19	5,3	4,12	1,1	15,18
Maximum value	39,15	7,06	8,83	6,47	1,63	21,49
Mean value	31,26	6,29	7,24	5,42	1,31	18,85
Standard deviation	4,18	0,42	0,79	0,47	0,12	1,57

Following the correlations between parameters assessed in the nonspecific chronic inflammation, we found that there is a strong correlation between: AN and P (0.8943 p<0.0001), AN and Deq (Deq r=0.9991 p<0.0001), AN and Dmax (r=0,7906 p<0,0001), AN and Dmin (r=0,6903 p<0,0001). Elongation does not correlate with nuclear area (r = 0.1737 p = 0.2713).

Tabel XCVI Comparison of mean values of parameters between solid adenocarcinoma and nonspecific chronic inflammation

morphometric parameter	**Lesion**		**t-test**
	Solid adenocarcinoma	nonspecific chronic inflammation	p value
nuclear area mean value (µm²)	72,45	31,26	p<0,0001
Mean diameter average value (µm)	9,55	6,29	p<0,0001
Maximus diameter average value (µm)	11,43	7,24	p<0,0001
Minimum diameter average value (µm)	8,14	5,42	p<0,0001
Elongation mean value	1,43	1,31	p=0,0003
Perimeter mean value (µm)	29,91	18,85	p<0,0001

By applying the t-test, we found that between nuclear parameters belonging to the two groups (solid adenocarcinomas and chronic nonspecific inflammation) are statistically significant differences (p <0.05). Thus, nuclear morphometry has proven useful in differentiating these lesions.

Table no. XCVII Comparison of average values of the parameters between nonspecific chronic inflammation and control group

morphometric parameter	**Lesion**	**t-test**

	Controls	ICN	p value
nuclear area mean value (µm²)	49,38	31,26	p<0,0001
Mean diameter average value (µm)	7,91	6,29	p<0,0001
Maximus diameter average value (µm)	9,32	7,24	p<0,0001
Minimum diameter average value (µm)	6,74	5,42	p<0,0001
Elongation mean value	1,32	1,31	p=0,8435
Perimeter mean value (µm)	24,02	18,85	p<0,0001

Differences between nuclear parameters characterizing nonspecific inflammation and control group are statistically significant, except elongation (p> 0.05).

Morphometric assessment of nonspecific granulomatous inflammation cases

Have been obtained the following nuclear parameters:

Table no. XCVIII Average values of nuclear parameters in nonspecific granulomatous inflammation

Nuclear values	AN (µm²)	Deq (µm)	Dmax (µm)	Dmin (µm)	E	P (µm)
Minimum value	27,37	5,9	6,47	4,71	1,1	17,72
Maximum value	35,68	6,74	7,65	5,89	1,5	19,78
Mean value	31,42	6,31	6,97	5,63	1,24	18,66
Standard deviation	3,29	0,33	0,4	0,46	0,12	0,82

Following the correlations between parameters assessed in the nonspecific granulomatous inflammation, we found that there is a strong correlation between: AN cu P (r=0,9871 p<0,0001), AN cu Deq (r=0,9997 p<0,0001). Nuclear area does not correlate with elongation (r = -0.2786 p = 0.5451), maximum diameter (r = 0.6793 p = 0.0933) and minimum diameter (r = 0.7388 p = 0.0578) .

Table no. XCIX Comparison of average values of the parameters between solid adenocarcinoma and nonspecific granulomatous inflammation

Morphometric parameter	**Lesion**		**t-test**
	Solid adenocarcinoma	nonspecific granulomatous inflammation	p value
Nuclear area mean value (µm²)	72,45	31,42	p=<0,0001
Mean diameter average value (µm)	9,55	6,31	p<0,0001
Maximus diameter average value (µm)	11,43	6,97	p<0,0001
Minimum diameter average value (µm)	8,14	5,63	p<0,0001
Elongation mean value	1,43	1,24	p=0,0049
Perimeter mean value (µm)	29,91	18,66	p<0,0001

Morphometric assessment of inflammatory pseudotumour case

Regarding this histopathological entity we obtained the following values of nuclear parameters:

Table no. CI: Nuclear parameter values for the inflammatory pseudotumour

Nuclear values	AN (μm^2)	Deq (μm)	Dmax (μm)	Dmin (μm)	E	P (μm)
Mean value	75,03	9,76	12,61	7,76	1,46	31,24

Average values of nuclear area in inflammatory pseudotumor are similar to those of solid adenocarcinomas and are about twice higher than those obtained in nonspecific chronic inflammation and nonspecific granulomatous inflammation.

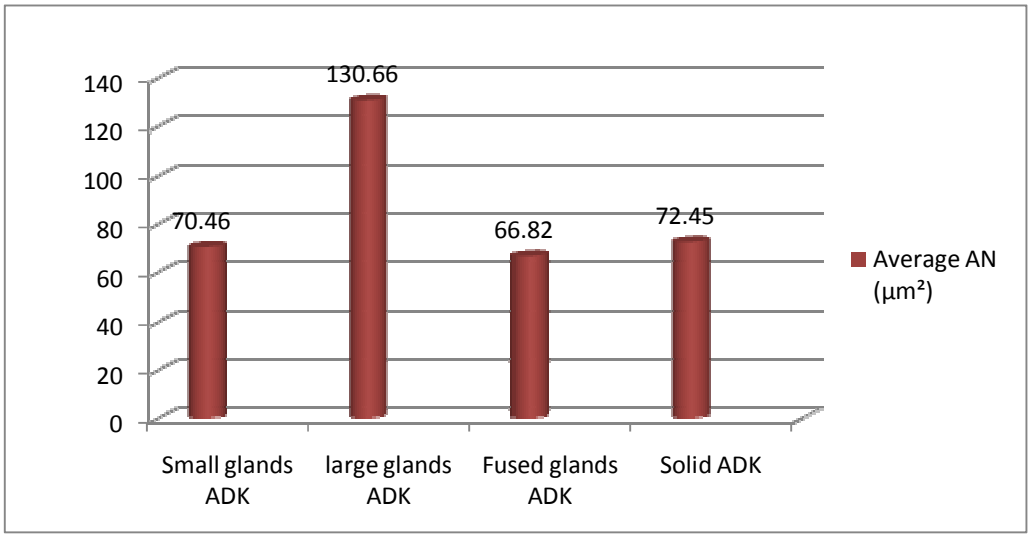

Figure 299 Mean nuclear area of adenocarcinomas based on glandular architecture

The method used was not sensitive enough to discriminate different Gleason grade adenocarcinomas, depending on glandular architecture. Thus, by comparing lots of adenocarcinoma, we identified statistically significant differences ($p < 0.05$) only between large gland adenocarcinoma group and all other groups (with small glands, fused and solid).

Elongation factor was not specific for adenocarcinomas with Gleason score known and thus had a low predictive value. It was not useful in differentiating any other injuries.

Conclusions

1). From the 1823 prostate lesions, adenocarcinomas were represented by 365 cases (20.02%), while lesions that mimic malignancy of 283 (15.52%), whose frequency increased progressively during the four years of study, dominated by the latter in 2011.
2). The distinction between adenocarcinomas and benign hyperplasia, proliferation of small glands, basal cell proliferation and prostate inflammation can not be made based on PSA. Following the comparative study to the average value of PSA, the results were statistically significant ($p < 0.05$) only between small glands adenocarcinomas with atrophy and Cowper glands and adenocarcinomas with the fused glands and xantogranulomatous inflammation.
3). Comparison of structural parameters between small gland adenocarcinomas and lesions that mimic malignancy showed that the results were statistically significant ($p < 0.05$) for the parameters represented by the diameter of the lesion, lobulated appearance, luminal contents, number of glands components. The presence of a central pseudoduct has been characteristic for atypical adenomatous hyperplasia, atrophy and Cowper glands. The presence of a periglandular halo and imunostaining for SMA were specific in case of sclerosing adenosis. The presence of basal cells was highlighted immunohistochemically using 34βE12 in lesions that mimic adenocarcinoma.
4). Immunohistochemically we noticed that differentiation of large gland adenocarcinomas from with cribriform clear cell hyperplasia was based on the 34βE12 immunostaining, which proved the presence of basal cell layer in clear cell hyperplasia and their absence in malignant neoplasia.
Differentiation between fused glands adenocarcinomas and xantogranulomatous inflammation was based on positive reaction to CD 68 and immunoreactions of malignant neoplasia to PSA.
Immunohistochemically, we found PSA positivity of solid adenocarcinomas, immunoreactivity for CD68 of nonspecific granulomatous inflammation and immunoreactivity for CD45 of chronic nonspecific inflammation. Inflammatory pseudotumor was negatively for PSA and vimentin positive.
5). Morphometric study performed on benign prostatic hyperplasia control group showed a average value for AN = 49.38 ± 5.7 μm ², similar to values obtained in normal prostate tissue studies published in international literature. This suggests that the action of hormonal stimulus results in increased number of glands, accompanied by cytonuclear changes. Nuclear morphometric parameters correlated closely ($0.5882 > r < 0.9994$), except elongation factor, which has a weak negative correlation type ($r = -0.2364$), but not statistically significant ($p > 0.05$).
6). For small gland adenocarcinomas, we obtained an average value of AN = 70.46 ± 16.85 μm², without reaching double nuclear area of controls. Nuclear area correlated with other morphometric parameters except elongation ($r = 0.09370$, $p = 0.4438$).
7). Morphometric evaluation of lesions that mimic small glands adenocarcinoma was established a strong correlation between the parameters evaluated, except elongation. Atypical adenomatous hyperplasia was characterized by values of AN = 58.11 ± 9.99 μm ², intermediate between the control group and that found in adenocarcinomas. Cowper glands and atrophy showed a nuclear area of 56.28 ± 4.36 μm² and 54.02 ± 6.42 μm ². The only lesion characterized by lower values of nuclear parameters compared with controls was sclerosing adenosis. Basal cell hyperplasia presents a nuclear area of 74.48 ± 14.57 μm², similar to small gland

adenocarcinomas and lower than bazaloid carcinoma (97.41 μm ²). In the elongation factor, it is not significantly different between benign and malignant lesions, while all other parameters were useful in discriminating the two types of lesions.

8). In case of large glands adenocarcinoma I found a mean nuclear area of 130.66 ± 27.97 μm ², almost three times higher than the control group, reflecting increased malignancy based on Gleason score. I noticed a strong correlation with other parameters of the nuclear area, except the minimum diameter and elongation.

In clear cell cribriform hyperplasia nuclear area had the average value 71.48 ± 5.26 μm².

9). Adenocarcinomas with fused glands presented AN = 66.82 ± 18.73 μm ², which correlated closely with all other parameters, except elongation (r = 0.03081 p = 0.8649). In the assessment xantogranulomatous inflammation nuclei, we obtained a mean nuclear area of 47.34 ± 8.52 μm².

10). For solid adenocarcinoma AN = 72.45 ± 9.97 μm ² was relatively similar to that obtained in small glands adenocarcinomas; the same features for other morphometric parameters. Between nuclear parameters was established strong correlations, except elongation factor. Nuclear area values in case of nonspecific granulomatous inflammation were 31.42 ± 3.29 μm², similar to those of chronic nonspecific inflammation (31.26 ± 4.18 μm²).

11). The complex histopathological, immunohistochemical and morphometric study comparison between adenocarcinomas and lesions that mimic malignancy showed that the differentiation is performed according to architectural aspects and allowed a histopathological diagnosis protocol:

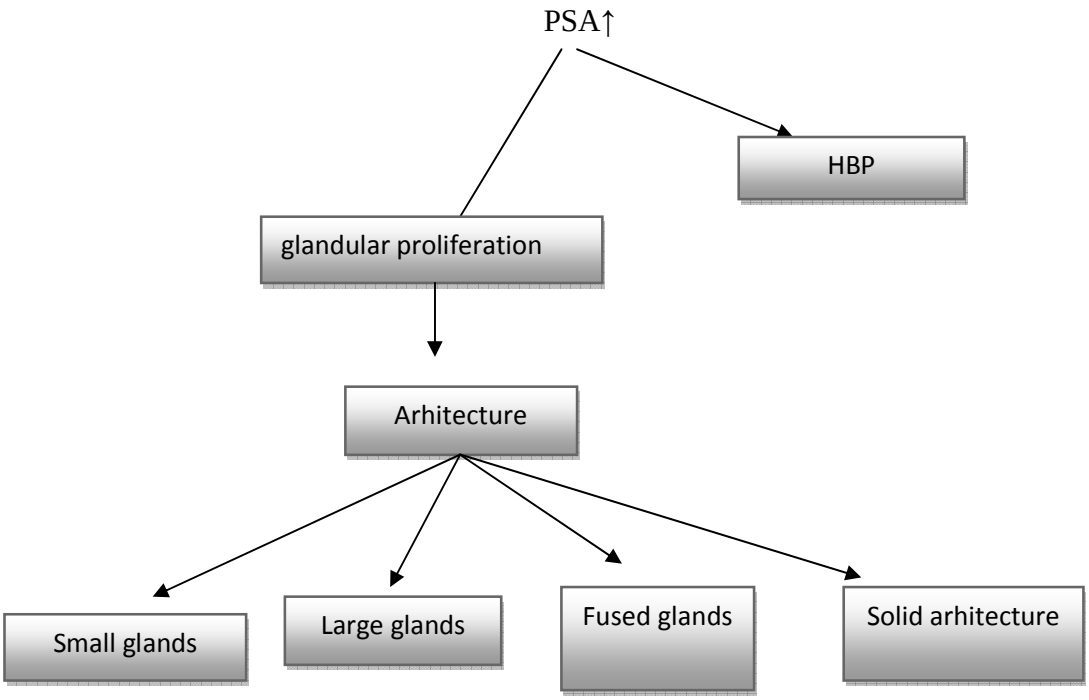

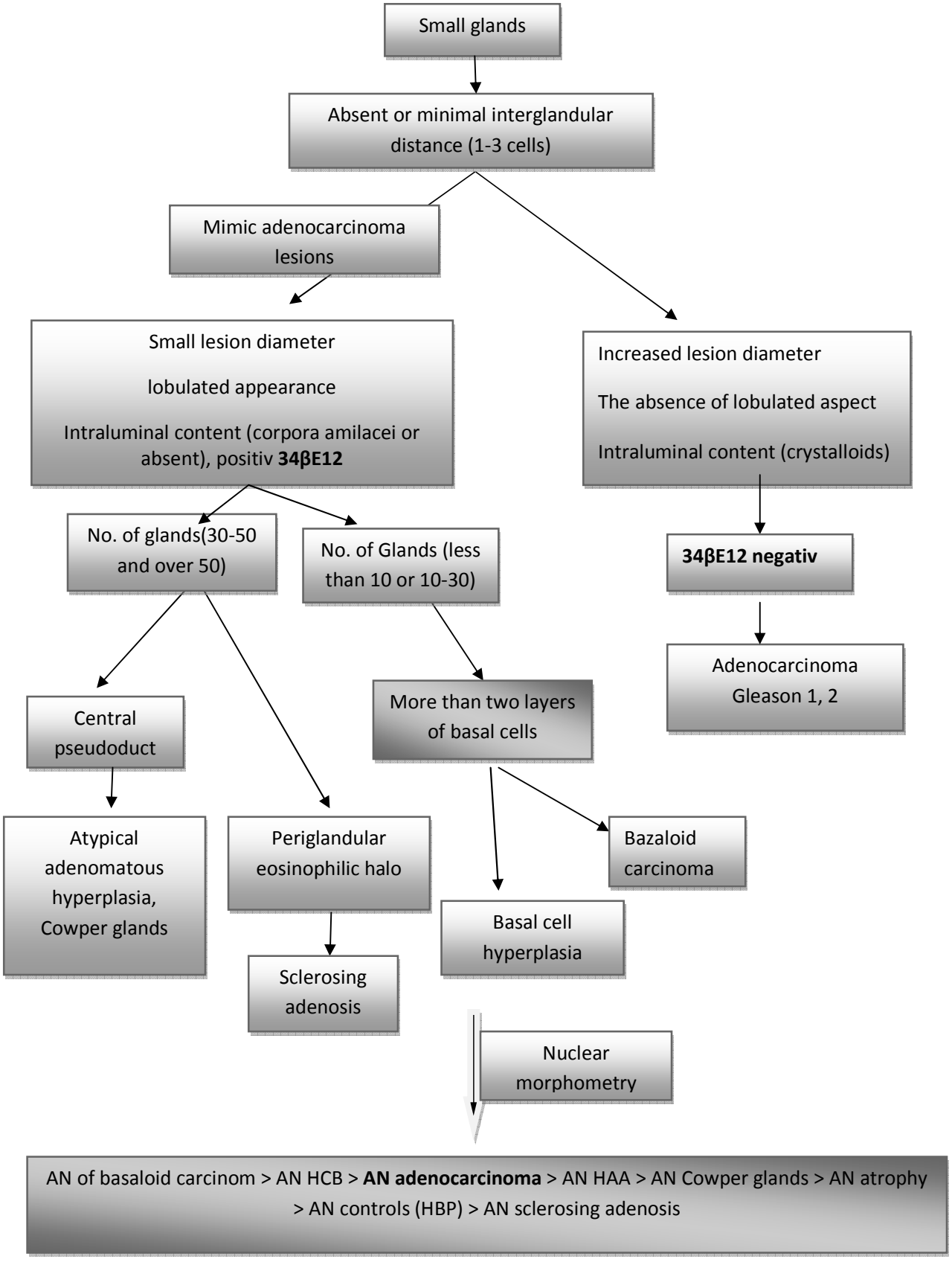
Small glands
Absent or minimal interglandular distance (1-3 cells)
Mimic adenocarcinoma lesions
Small lesion diameter
lobulated appearance
Intraluminal content (corpora amilacei or absent), positiv **34βE12**
Increased lesion diameter
The absence of lobulated aspect
Intraluminal content (crystalloids)
No. of glands(30-50 and over 50)
No. of Glands (less than 10 or 10-30)
34βE12 negativ
Adenocarcinoma Gleason 1, 2
Central pseudoduct
More than two layers of basal cells
Atypical adenomatous hyperplasia, Cowper glands
Periglandular eosinophilic halo
Bazaloid carcinoma
Basal cell hyperplasia
Sclerosing adenosis
Nuclear morphometry
AN of basaloid carcinom > AN HCB > **AN adenocarcinoma** > AN HAA > AN Cowper glands > AN atrophy > AN controls (HBP) > AN sclerosing adenosis

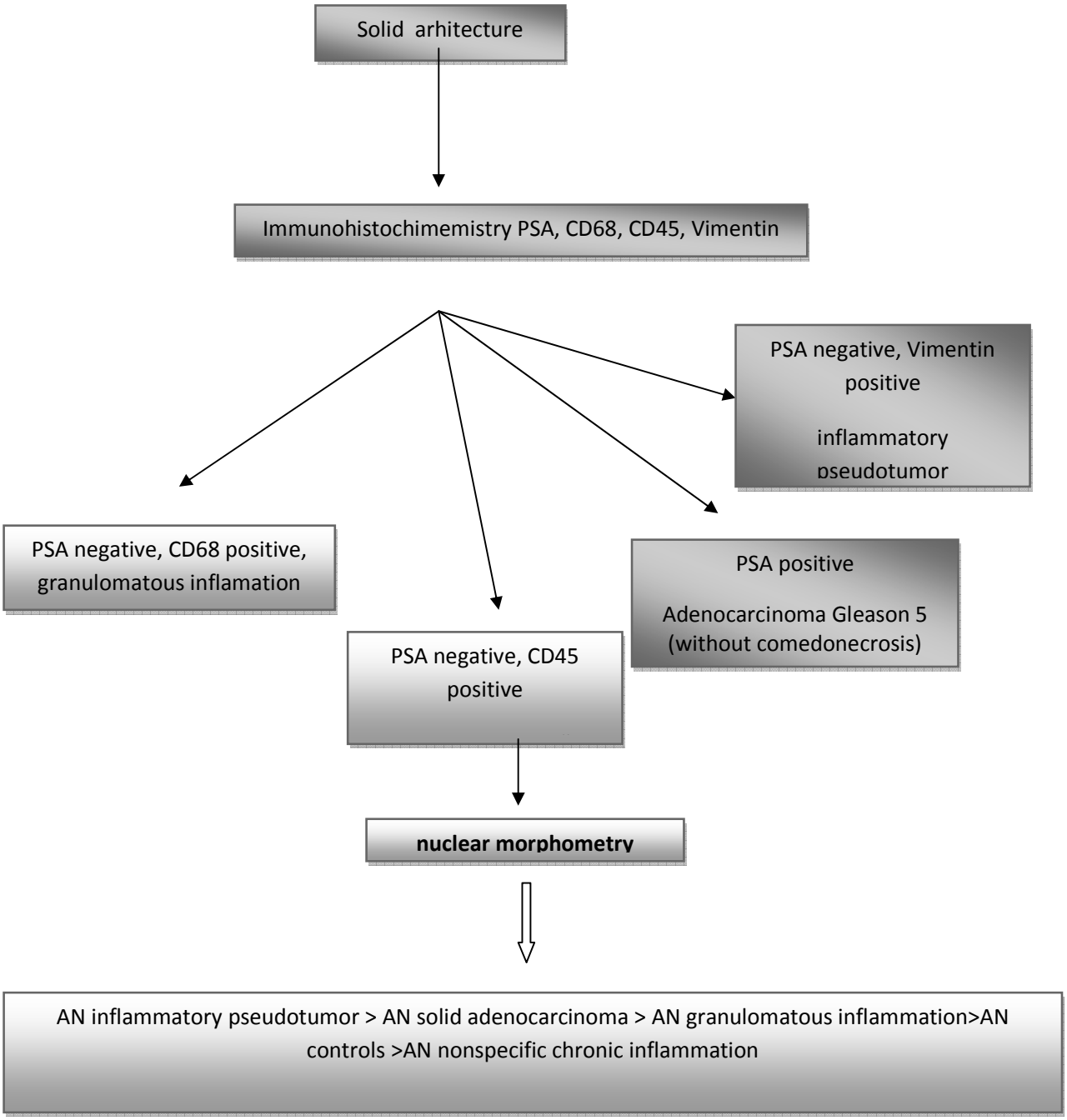
Solid arhitecture
Immunohistochimemistry PSA, CD68, CD45, Vimentin
PSA negative, Vimentin positive
inflammatory pseudotumor
PSA negative, CD68 positive, granulomatous inflamation
PSA positive
Adenocarcinoma Gleason 5 (without comedonecrosis)
PSA negative, CD45 positive
nuclear morphometry
AN inflammatory pseudotumor > AN solid adenocarcinoma > AN granulomatous inflammation>AN controls >AN nonspecific chronic inflammation

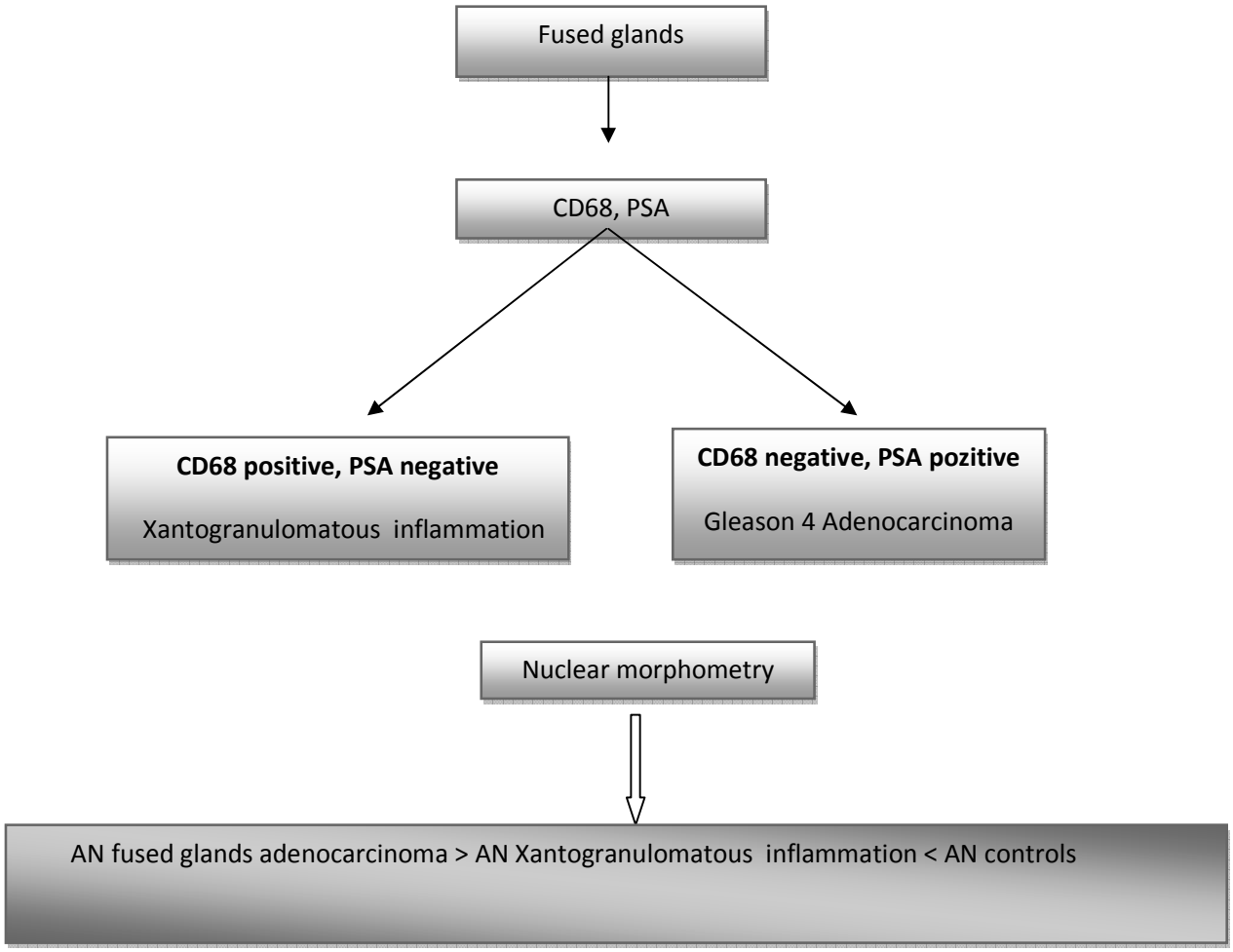
Fused glands
CD68, PSA
CD68 positive, PSA negative
Xantogranulomatous inflammation
CD68 negative, PSA pozitive
Gleason 4 Adenocarcinoma
Nuclear morphometry
AN fused glands adenocarcinoma > AN Xantogranulomatous inflammation < AN controls

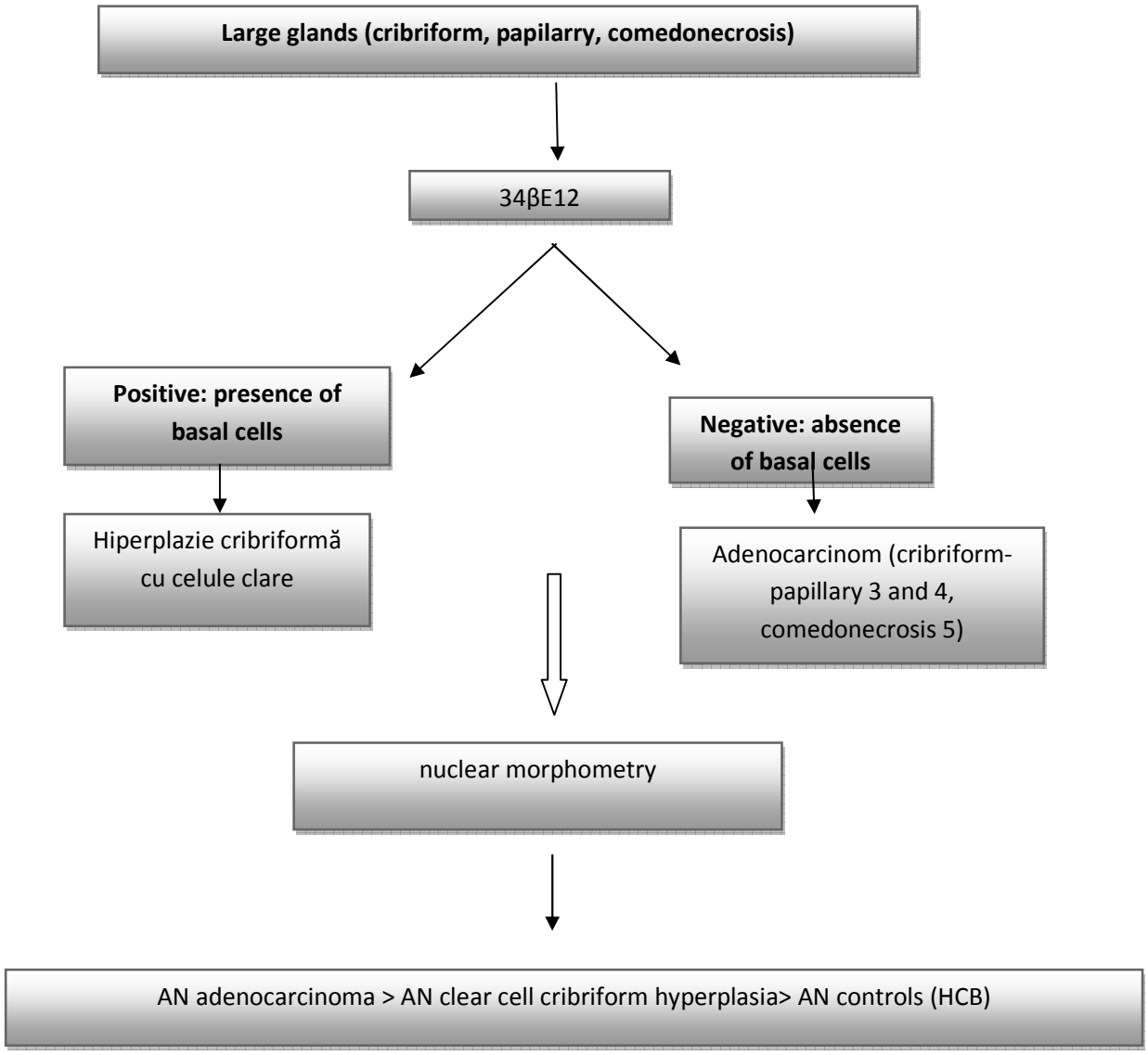
Large glands (cribriform, papilarry, comedonecrosis)
34βE12
Positive: presence of basal cells
Negative: absence of basal cells
Hiperplazie cribriformă cu celule clare
Adenocarcinom (cribriform-papillary 3 and 4, comedonecrosis 5)
nuclear morphometry
AN adenocarcinoma > AN clear cell cribriform hyperplasia> AN controls (HCB)

Selective bibliography

1. Gleason DF. Classification of prostatic carcinoma. Cancer Chemother Rep 1996; 50:125-128
2. Gleason DF. Histologic grading and clinical staging of prostatic carcinoma In: The prostate. Lea &Febiger: Philadelphia, 1977, pp. 171-197
3. Srigley JR. Benign mimickers of prostatic adenocarcinoma. Modern Pathology, 2004; 17: 328-348
4. Epstein JI, Allsbrook W C Jr, Amin M B et al. 2005 The 2005 International Society of Urologic Pathology (ISUP) consensus conference on Gleason grading of prostatic carcinoma, Am J Surg Pathol 29:1228-1242
5. Mogoanţă L, Georgescu CV, Popescu CF, Bădulescu A, Mehedinţi Hîncu M. Guide of histology techniques, cytology and immunohistochemistry. Craiova, the Medical University Ed , 2003
6. www.dako.com
7. Rosai J, Rosai and Akerman's Surgical Pathology, chapter 18, Male reproductive system, Mosby, Philadelphia, 2004, 1386-87
8. Fletcher CDM, Diagnostic Histopathology of Tumors, Third Edition, first volume, Churchill Livingstone, Elsevier, 2007, 749-811
9. Midi A, Tecimer T, Bozkurt S, Ozkan N. Differences in the structural features of atypical adenomatous hyperplasia and low-grade prostatic adenocarcinoma, Indian Journal of Urology, 2008, 24(2):169-177
10. Gaudin PB, Epstein JI. Adenosis of the prostate. Histologic features in transurethral resection specimens, Am J Surg Pathol 1994;18: 863-870
11. Bostwick OG, Srigley J, Grignon DJ, et al. Atypical adenomatous hyperplasia of the prostate: morphologic criteria for its distinction from well-differentiated carcinoma. Hum Pathol. 1993;24:819-832
12. Cohen RJ, McNeal JE, Redmond SI et al. Luminal contents of benign and malignant prostatic glands: Corespondence altered secretory mechanisms. Hum Pathol 2000;31: 94-100
13. Cheng L, Bostwick DG. Atypical sclerosing adenosis of the prostate: a rare mimic of adenocarcinoma Histopathology 2010, 56:627-631
14. Meister P. Sclerosing adenosis of the prostate: carcinoma simulation. Pathologie, 1996, Mar. 17(2):157-62

15. Jones EC, Clement PB, Young RH. Sclerosing adenosis of the prostate gland. A clinicopathological and immunohistochemical study of 11 cases. Am J Surg Pathol 1991; 15: 1171-1180
16. Billis A: Prostatic atrophy: an autopsy study of a histologic mimic of adenocarcinoma. Mod Pathol 1998; 11: 47-54
17. Cina SJ, Silberman MA, Kahane H, et al. Diagnosis of Cowper's glands on prostate needle biopsy. Am J Surg Pathol 1997; 21: 550-555
18. Saboorian MH, Huffman H, Ashfaq R et al. Distinguishing Cowper's glands from neoplastic and pseudoneoplastic lesions of prostate. Immunohistochemical and ultrastructural studies. Am J Surg Pathol 1997; 21: 1069-1074
19. Srigley JR. Small acinar patterns in the prostate gland with emphasy on atypical adenomatous hyperplasia and small acinar carcinoma. Semin Diagn Pathol 1988:5: 254-272
20. Bryan RL, Newman J, Campbell A. Granulomatous prostatitis. A clinicopathological study. Histopathology. 1991; 9:453-457 (**91**)
21. Price H, McNeal JE, Stamey TA. Evolving patterns of tissue composition in benign prostate hyperplasia as a function of specimen size. Hum Pathol 1990; 21: 578-85
22. Eri LM, Svindland A. Can prostate epithelial content predict response to hormonal treatment of patients with benign prostatic hyperplasia? Urology 2000; 56: 261-6
23. Barstch G, Muller HR, Oberholzer M. et al. Light microscopic stereological analysis of the normal human prostate and of benign prostatic hyperplasia. J Urol 1979; 122: 487-91
24. Chagas MA, Babinski MA, Costa WS, Sampaio FJB. Stromal and acinar components of the transition zone in normal and hyperplastic human prostate. BJU Int 2002; 89: 699-702
25. Wang N, Stenkvist BG, Tribukait B, Morphometry of nuclei of the normal and malignant prostate in relation to DNA ploidy. Analytical and Quantitative Cytology and Histology/the International Academy of Cytology and American Society of Cytology 1992, 14(3):210-216
26. Taboga SR, Dos Santos AB, Gonzatti AGR, Vidal BC, Mello MLS. Nuclear phenotypes and morphometry of human secretory prostate cells: a comparative study of benign and malignant lesions in Brazilian patients, Caryologia,2003, vol. 56, 3:315-322
27. Shapiro E, Hartanto V, Periman EJ. Et al. Morphometric analysis of pediatric and nonhyperplasic prostate glands: evidence that BPH is not a unique stromal process. Prostate 1997; 33: 177-182

28. Montironi R, Mazzacchelli R, Stramazzoti D, Scarpelli M, Lopez Beltran A, Bostwick DG. Basal cell hyperplasia and basal cell carcinoma of the prostate: a comprehensive review and discussion of a case with c-erbB-2 expression, J Clin Pathol 2005; 58: 290-296
29. Choi NG, Sohn JH, Park HW. And Jung TY, 1999 – Apoptosis and nuclear shapes in benign prostate hyperplasia and prostate adenocarcinoma: comparison with and relation to Gleason score. Int J Urol 6: 13-18